

AD-A064 328

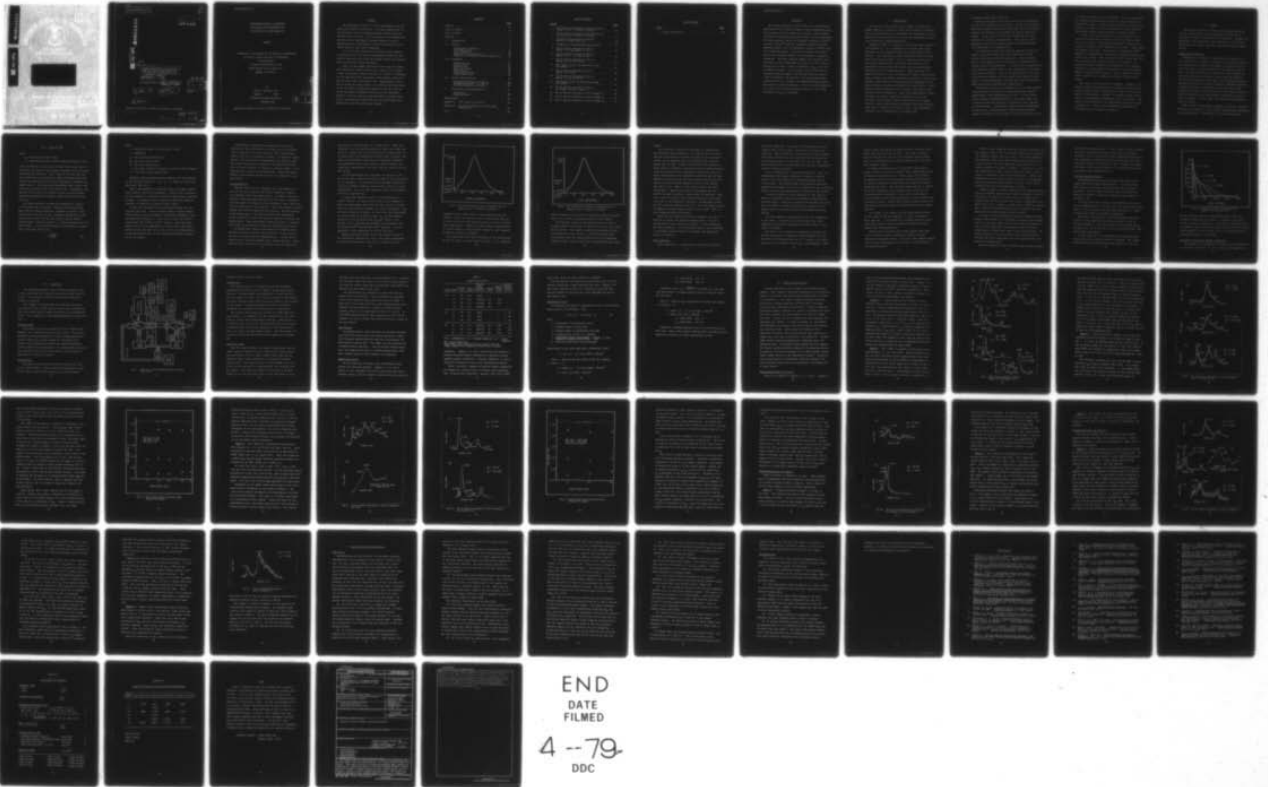
AIR FORCE INST OF TECH WRIGHT-PATTERSON AFB OHIO SCH--ETC F/G 20/12
CATHODOLUMINESCENCE OF GERMANIUM IMPLANTED GALLIUM ARSENIDE AND--ETC(U)
DEC 78 J H WALCHER

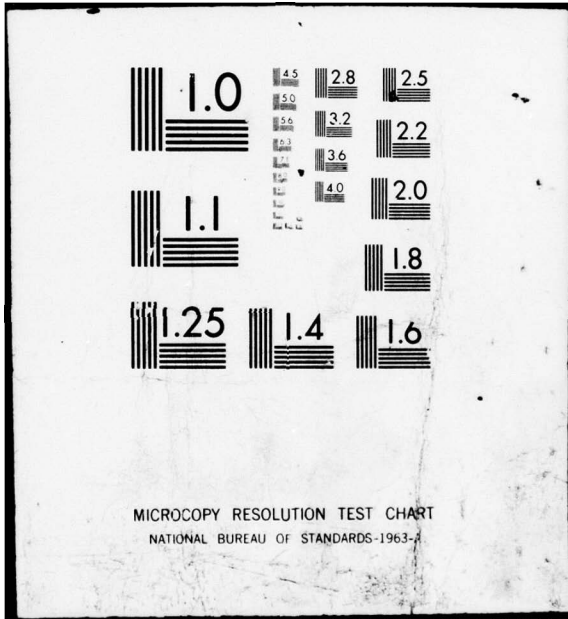
UNCLASSIFIED

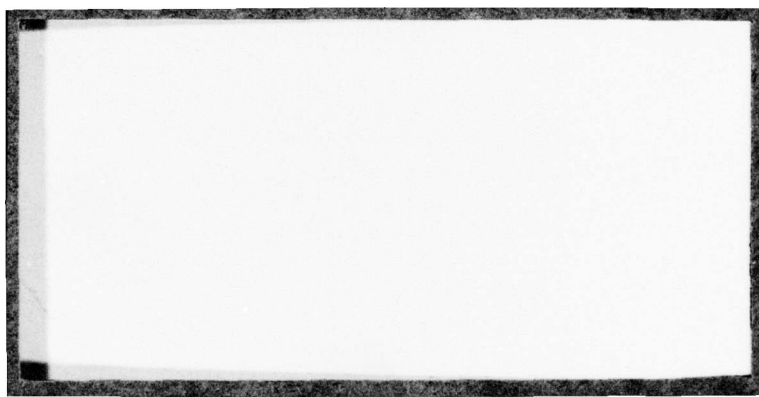
AFIT/GEP/PH/78D-16

NL

1 OF 1
AD
A064 328







14

AFIT/GEP/PH/78D-16

①

LEVEL II

ADA 064328

DDC FILE COPY

⑥

CATHODOLUMINESCENCE OF GERMANIUM
IMPLANTED GALLIUM ARSENIDE AND
THE EFFECTS OF LASER ANNEALING.

⑨ Masters THESIS

⑩

AFIT/GEP/PH/78D-16 James H. Walcher
Captain USAF

DDC
FEB 8 1979
A

⑪ Dec 78

⑫ 75 p.

⑬ 2306

Approved for public release; distribution unlimited.

611 0 27

012 225

79 01 30 122

Act

CATHODOLUMINESCENCE OF GERMANIUM
IMPLANTED GALLIUM ARSENIDE AND
THE EFFECTS OF LASER ANNEALING

THESIS

Presented to the Faculty of the School of Engineering
of the Air Force Institute of Technology
Air University
in Partial Fulfillment of the
Requirements for the Degree of
Master of Science

by

James H. Walcher, B.S.

Captain USAF

Graduate Engineering Physics

December 1978

CLASSIFICATION	GROUP 1	<input checked="" type="checkbox"/>
GROUP 2	GROUP 3	<input type="checkbox"/>
GROUP 4	GROUP 5	<input type="checkbox"/>
GROUP 6	GROUP 7	<input type="checkbox"/>
GROUP 8	GROUP 9	<input type="checkbox"/>
DISTRIBUTION AVAILABILITY CODES		
INTL	AVAIL	EXC/SPC/AL
A		

Approved for public release; distribution unlimited.

Preface

The importance of GaAs as a III-V semiconductor and its derivatives cannot be overrated. Its future applications in the microwave and the telecommunications industry have not yet been fully realized. With the advent of ion implantation and the present experimental research advances in laser annealing, GaAs is guaranteed a very strong foothold in our future world of solid-state technology.

It is a distinct honor for me to present this study as my contribution to the present experimental research on GaAs with the hope that this study may someday enhance the progress made in the field of GaAs technology.

There are many people who gave up their time and energy, thus making this study possible, that I would like to thank. I want to especially thank my advisor, Dr. Robert L. Hengehold, for the many useful and informative conversations during the course of this most interesting work. Additionally, I owe a debt of thanks to George Gergal, Jim Miskimen, and Ron Gabriel of the AFIT Physics Department technical staff for their untiring assistance throughout the period of the experiment. Finally, I wish to record my deep gratitude to Suzanne Weber for her many valuable suggestions and her outstanding job in helping me to put this manuscript together.

Contents

	<u>Page</u>
Preface	ii
List of Figures	iv
List of Tables	v
Abstract.	vi
I. Introduction.	1
II. Theory.	4
Luminescence Mechanisms	4
Ion Implantation.	9
Laser Annealing	13
Electron Beam Penetration	17
Impurities and Lattice Vacancy Competition.	18
III. Experiment.	21
Cooling System.	21
Vacuum System	21
Electron Gun.	23
Detection System.	23
Data Display.	24
Sample Description.	24
Experimental Error.	26
IV. Results and Discussion.	28
Cathodoluminescence of Group #1	28
Cathodoluminescence of Group #2	42
Cathodoluminescence of Group #3	45
V. Conclusions and Recommendations	52
Conclusions	52
Recommendations	56
Bibliography.	58
Appendix A: GaAs Values of Interest.	63
Appendix B: Various Estimates of Electron Beam Penetration.	64
Vita.	65

List of Figures

<u>Figure</u>	<u>Page</u>
1 LSS Profile of Germanium Implanted GaAs of Fluence 3×10^{13} Ions/cm ² at 120 keV.	11
2 LSS Profile of Germanium Implanted GaAs of Fluence 3×10^{14} Ions/cm ² at 120 keV.	12
3 Estimated Electron Beam Excitation Profiles in GaAs (Ref 12)	18
4 Schematic of Cathodoluminescence System	22
5 The CL Spectra Obtained at 10°K on Sample 1 (a) and Sample 2 (b-d)	30
6 The CL Spectra Obtained at 10°K on Sample 3 at 5, 7.5, and 10 keV.	32
7 The CL Spectra Obtained at 10°K on Sample 3 at 13 and 15 keV	33
8 Peak Energy Versus Electron Beam Energy for Sample 3.	36
9 The CL Spectra Obtained at 10°K on Sample 4 at 5 keV	38
10 The CL Spectra Obtained at 10°K on Sample 4 at 10 and 15 keV	39
11 Peak Energy Versus Electron Beam Energy for Sample 4.	40
12 The CL Spectra Obtained at 10°K on (a) Sample 5 and (b) Sample 6	43
13 The CL Spectra Obtained at 10°K on Sample 8	46
14 The CL Spectra Obtained at 10°K on Sample 9	48
15 The CL Spectra Obtained at 10°K on Sample 10.	51

List of Tables

<u>Table</u>		<u>Page</u>
I	Sample Description	25

Abstract

The primary objective of this study was to characterize experimental laser annealed samples using cathodoluminescence. Ten Cr-doped (SI) GaAs samples were studied. These samples included an unimplanted-unannealed sample, several unimplanted but laser annealed samples, Ge implanted (fluences of 3×10^{13} ions/cm² and 3×10^{14} ions/cm²) thermally annealed and laser annealed samples, and a Ge implanted (fluence of 3×10^{14} ions/cm²) unannealed sample. The results indicated the experimental laser annealed samples to be partially or completely unannealed. The laser annealed samples were generally characterized by weak luminescence with peaks at 1.514 eV due to unresolved excitons, 1.488 eV attributed to Zn_{As}, and 1.469 eV (damage related). It was further observed that in the thermally annealed samples, the dominant peak was noted at 1.488 eV instead of the expected 1.478 eV peak previously associated with Ge. Finally, the unannealed sample spectra emissions were characterized by a 1.493 eV peak attributed to C_{As}, and in all non-laser annealed samples a 1.36 eV peak attributed to Cu_{Ga} was observed.

I. Introduction

The purpose of this study was to examine the effects of damage induced in a gallium arsenide (GaAs) sample by germanium (Ge) ion implantation and to determine the consequences of laser annealing on these effects by utilizing the experimental laboratory technique of cathodoluminescence.

Gallium arsenide is a group III-V direct gap semi-conductor (see Appendix A). It is zincblende in structure and can be considered as two interpenetrating face-centered-cubic (FCC) lattices. This material has been extensively studied for many years for two main reasons. First, it possesses unique properties that make possible significant improvements in the performance of many electronic devices such as photocathodes. Properties such as higher mobilities, larger band gap, and a higher resistivity or semi-insulating (SI) quality make possible higher frequency and higher temperature operation of such devices. Secondly, GaAs exhibits interesting physical phenomena such as higher frequency electrical instabilities (Gunn effect). These phenomena have enhanced both the electrical and optical applications of GaAs tremendously. Today these applications include microwave oscillators, amplifiers, detectors, ultra fast switches, logic elements, infrared photoemitters, secondary emitters, light-emitting diodes and lasers, and high efficiency solar cells. Clearly, the future of GaAs is very promising, especially for its application to microwave and

telecommunications (Ref 2:129; 24).

Recently new emphasis has been placed on the investigation of GaAs by the United States Air Force. The Air Force Avionics Laboratory, Wright-Patterson Air Force Base, Ohio, is presently studying ion implantation experiments of various doped GaAs samples. These studies are directly related with Air Force interests in microwave communications. This present study is designed to provide new information on the implantation and laser annealing of Ge implanted GaAs.

Ion implantation offers an alternate approach to the diffusion of desired elements into GaAs substrates to yield desired electrical and optical properties. Laser annealing offers a new approach to the elimination of unwanted defects induced during ion implantation. In total, the ion implantation-laser annealing process offers a new, rapid method of assembly line device production. With the rising demand for GaAs doped with different elements, the ion implant-laser anneal process offers a distinct advantage of holding down costs considerably while shortening processing time significantly.

Pure GaAs, as well as ion implanted GaAs, has been examined using the optical techniques of photoluminescence, electroluminescence, and cathodoluminescence (CL). In this study, depth resolved cathodoluminescence is used since little work to date has been done using this technique on laser annealed Ge implanted GaAs. Additionally, depth resolved cathodoluminescence offers a unique method of investigating implanted samples at different crystal depths without etching away layers

as required by other optical techniques. This is accomplished by varying the accelerating potential of the electrons bombarding the sample. Through a careful analysis of the emitted spectra, one should be able to characterize crystal implants and probable implant concentrations at different depths.

In this study ten GaAs samples were investigated at pre-selected probing depths using an electron beam energy range of 5 keV to 15 keV. Two thermally annealed Ge implanted GaAs samples of fluences 3×10^{14} ions/cm² were studied. These samples were capped with Si₃N₄. Additionally, an unannealed 3×10^{14} ions/cm² Ge implanted GaAs sample and an unannealed-unimplanted sample were studied. These provided the basis group from which the succeeding laser annealed samples were compared. The succeeding samples included three unimplanted laser annealed chromium (Cr) compensated GaAs substrates, one laser annealed sample of fluence 3×10^{14} ions/cm², and two samples of fluence 3×10^{13} ions/cm² laser annealed at different energy density values.

This study is divided into five chapters. Chapter II contains the theory and previous work accomplished necessary for careful interpretation of experimental results as well as for support of conclusions. Chapter III contains a brief description of the experimental arrangement used in this study. The analysis and discussion of the experimental results are found in Chapter IV. Finally, some interesting conclusions and recommendations are located in Chapter V.

II. Theory

This section contains the theory and background necessary for the interpretation of the experimental results and the conclusions reached. The major areas covered are: luminescence mechanisms, ion implantation, laser annealing, electron beam penetration, and finally impurities and lattice vacancy competition.

Luminescence Mechanisms

Luminescence is defined as "the emission of optical radiation (ultraviolet, visible, or infrared) as a result of electronic excitation of a material, excluding any radiation which is the result purely of the temperature of the material" (Ref 50: 626). The optical radiation is produced by the recombination of electron-hole pairs created by some excitation mechanism. The excitation mechanisms used today include photoluminescence, involving excitation via optical radiation; cathodoluminescence, in which excitation is provided by an electron beam; radioluminescence, which induces excitation by high-energy radiation; and electroluminescence, which induces excitation by electric field or current. In this study, the method of cathodoluminescence was chosen.

When a sample is bombarded by energetic electrons, electron-hole pairs are produced. These quickly recombine both radiatively and non-radiatively. Radiatively, the electron-hole pairs

recombine in GaAs via two major mechanisms of interest. They are conduction band to acceptor level recombinations (F-B) and donor level to acceptor level recombinations (D-A). These radiative recombination mechanisms arise from the presence of chemical impurities (intentionally or unintentionally put in the crystal) and physical defects (lattice vacancies, etc.). In addition to the mechanisms mentioned, other interband radiative recombination mechanisms exist. These are of lesser importance but are mentioned since they are found in the spectra of GaAs. They are excitons and phonons.

Much has been written on the subject of (F-B) recombination theory (Ref 5:6-7; 12:96-98; 40:39-40). The energy associated with such a recombination is approximated by the equation:

$$E = E_G - E_B + KT \pm nE_p \quad (1)$$

where

E = energy of free-bound transition

E_G = band gap energy

E_B = acceptor binding energy

K = Boltzmann's constant

T = temperature

n = integral number (0, 1, 2, 3...)

E_p = phonon energy

E_G represents the band gap energy which is temperature dependent and can be approximated by the equation (Ref 51:24):

$$E_G(T) = E_G(0) - \frac{aT^2}{T+b} \quad (2)$$

where

$$\begin{aligned}E_G(0) &= 1.522 \\ a &= 5.8 \times 10^{-4} \\ b &= 300\end{aligned}$$

Since the experimental data in this study is taken at 10°K, the KT term in Eq (1) is negligible. The $\frac{+nE_p}{p}$ term represents the number of phonons. For GaAs, longitudinal optical (LO) phonons have an approximate energy of 36 meV (Ref 49:2450).

The donor-acceptor (D-A) recombination theory has also been widely discussed (Ref 13:84; 40:40-41). This mechanism, in which an electron bound to a donor impurity recombines with a hole bound to an acceptor impurity, is described by the following equation:

$$E = E_G - (E_A + E_D) + \frac{e^2}{kR} \quad (3)$$

where

- E = energy of (D-A) transition
- E_G = band gap energy
- E_A = acceptor activation energy
- E_D = donor activation energy
- e = electron charge
- k = static dielectric constant
- R = separation distance

When employing Eq (3), one must consider the radiative recombination (transition) rates $W(r)$ approximated by the equation (Ref 13:85):

$$W(r) = W_{\max} \exp\left(-\frac{r}{r_D}\right) \quad (4)$$

where

r_D = half the donor Bohr radius

r = separation distance between donor and acceptor sites

Since transitions of near pairs are more likely than those of far pairs, the spectral peak energies increase as one increases the excitation intensity. This is due to the fact that near pair transitions are saturated at high excitation intensities so that the peak energy of the pair continuum is displaced to higher energy. Time-resolved cathodoluminescence studies have been used to examine such shifts (Ref 6:10). Furthermore, the spectra of near pairs are narrower because they have higher transition probabilities (shorter transition times) than the far pairs.

The final radiative recombination mechanism of interest is the production of excitons. Excitons are electron-hole pairs that are bound together by coulombic attraction. Some excitons are free and, as such, propagate through the crystal lattice while other excitons are bound to neutral donors, ionized donors, neutral acceptors, or ionized acceptors (Ref 23: 464; 45:4577). The ionization energy of an intrinsic exciton can be expressed (Ref 41:9) as

$$G = \frac{13.6\mu}{m\epsilon^2 n^2} \quad (5)$$

where

G = ionization energy of an intrinsic exciton

$$\mu = m_e m_h / m_e + m_h$$

m_e = the electron effective mass

m_h = the hole effective mass

m = the free electron mass

ϵ = the static dielectric constant of the host semi-conductor

$n = 1$ for the exciton ground state

Therefore, the excitation energy necessary for the creation of the intrinsic exciton is $E_{ex} = E_G - G$ where E_G is the band gap energy (Ref 41:9).

When a semiconductor is doped with donor or acceptor impurities, impurity levels are introduced. A donor level is defined as being neutral if filled by an electron, and positive (ionized) if empty. An acceptor level is neutral if empty and negative (ionized) if filled by an electron (Ref 51:626).

In GaAs free excitons have an approximate energy of 1.515 electron volts (eV). Those excitons, bound to neutral donors, ionized donors, neutral acceptors, and ionized acceptors, yield the approximate energies of 1.514, 1.513, 1.512, and 1.502 eV respectively (Ref 23:464; 45:4577; 56:345). Since the experimental error of this experiment is of the order ± 1 meV (milli electron volt), the best that can be said in the interpretation of the experimental data is that unresolved excitons are observed in the spectra.

Non-radiative recombination mechanisms are the least understood. Since they offer no insight into the concentration of impurities or lattice defects, these non-radiative centers will not be considered in depth. It should be stated, however, that a decrease in luminescence can indicate, under the proper conditions, an increase in non-radiative centers. This, in turn, indicates an increase in crystal damage--a most important part of spectra interpretation. Beyond this point, however, non-radiative centers will not be considered in any more detail.

Ion Implantation

Impurity atoms must be introduced into semiconductors to gain the desired electrical and optical properties required for different solid state applications. To achieve this goal, diffusion techniques have been used over the years. Diffusion consists mainly of diffusing a desired impurity into a wafer and the redistribution of that impurity. There are problems involved, though, that greatly complicate this process. The distribution of the doping agent is not always uniform and reproducible. Localizing defects result from chemical reactions involving the doping agents. Some applications require low doses--a variable that cannot be controlled by diffusion techniques (Ref 14:53).

Ion implantation offers an alternative to diffusion and a possible solution to some of these problems. First, a word is in order as to just what ion implantation is. In the ion implant process, ions are produced from a source material. These ions are then extracted electrostatically from the source and

directed in a uniform manner at a target wafer. Under the influence of an accelerating potential, these ions impact the wafer in a manner that has been described by Gibbons (Ref 20). As noted above, the implantation process offers possible solutions to the problems associated with diffusion techniques. Ion implantation offers dose control, profile control, low temperature implantation, and simple impurity sources (Ref 18: 295; 44:32).

An ion implantation unit integrates the current to the wafer and, thus, achieves an accurate count of the total number of ion implanted. If the neutrals and secondary charged particles are handled correctly, accurate dose control is easily accomplished. This is a most important aspect in the application of ion implantation.

A second most important aspect of ion implantation is profile control. So long as the crystal is not aligned in a major crystallographic direction with the ion beam, profiles resulting from different implants are easily reproduced. They are nearly Gaussian in shape. As such, they can be described by a mean called the projected range, R_p , and the standard deviation of the projected range ΔR_p (Ref 18:304-7; 20). Figures 1 and 2 represent the profiles of Ge implanted GaAs of fluences 3×10^{13} ions/cm² and 3×10^{14} ions/cm². All were implanted at room temperature at 120 keV (Ref 20).

Another advantage offered by the ion implant process is low temperature implantation, that is the sample temperature at which the implantation took place. Normally ions are

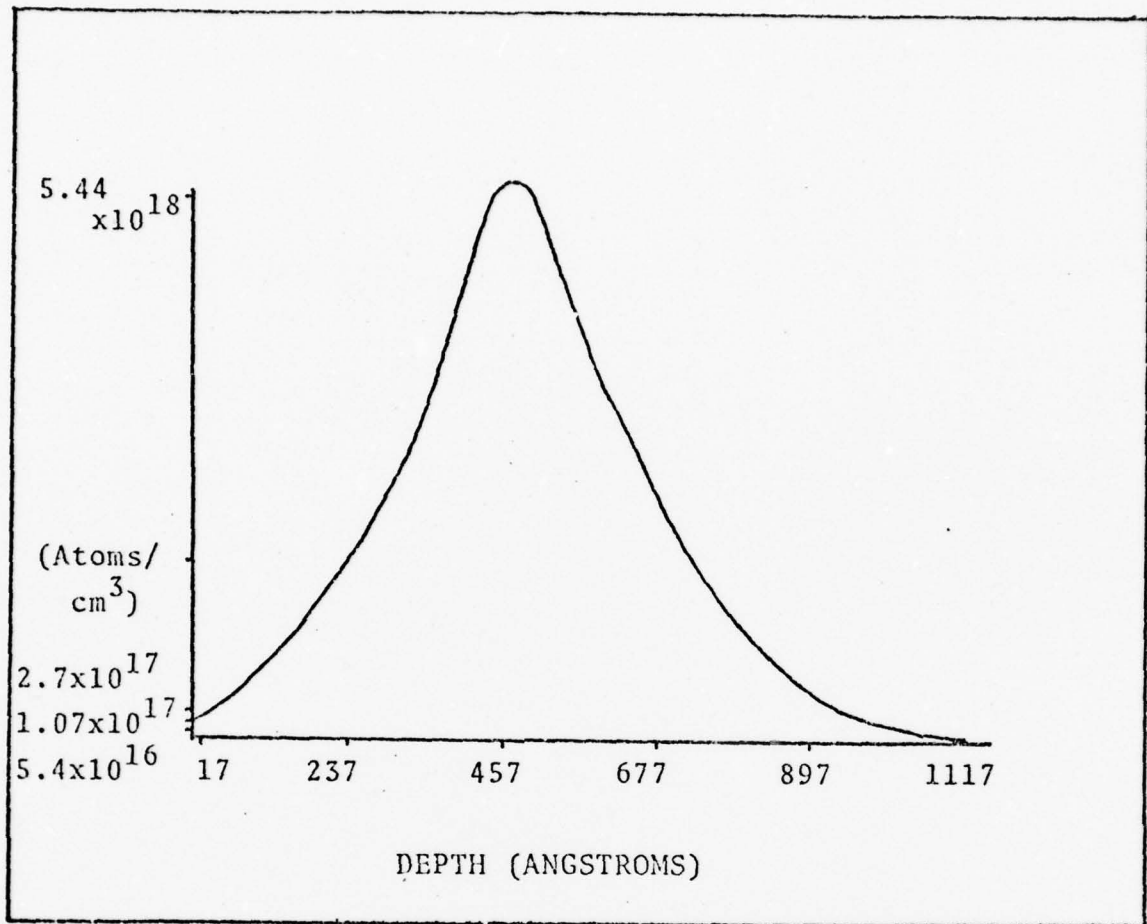


Fig 1. LSS Profile of Germanium Implanted GaAs of Fluence 3×10^{13} Ions/cm² at 120 keV

implanted into a sample held at room temperature for two reasons. First, the material used to selectively mask part of the wafer against the implant need not be able to survive high temperatures. Second, the total impurity concentration at various depths is significantly changed so that unwanted diffusion is held to a minimum.

The fourth and final major advantage of ion implantation is that it offers a simple impurity source. It is sometimes

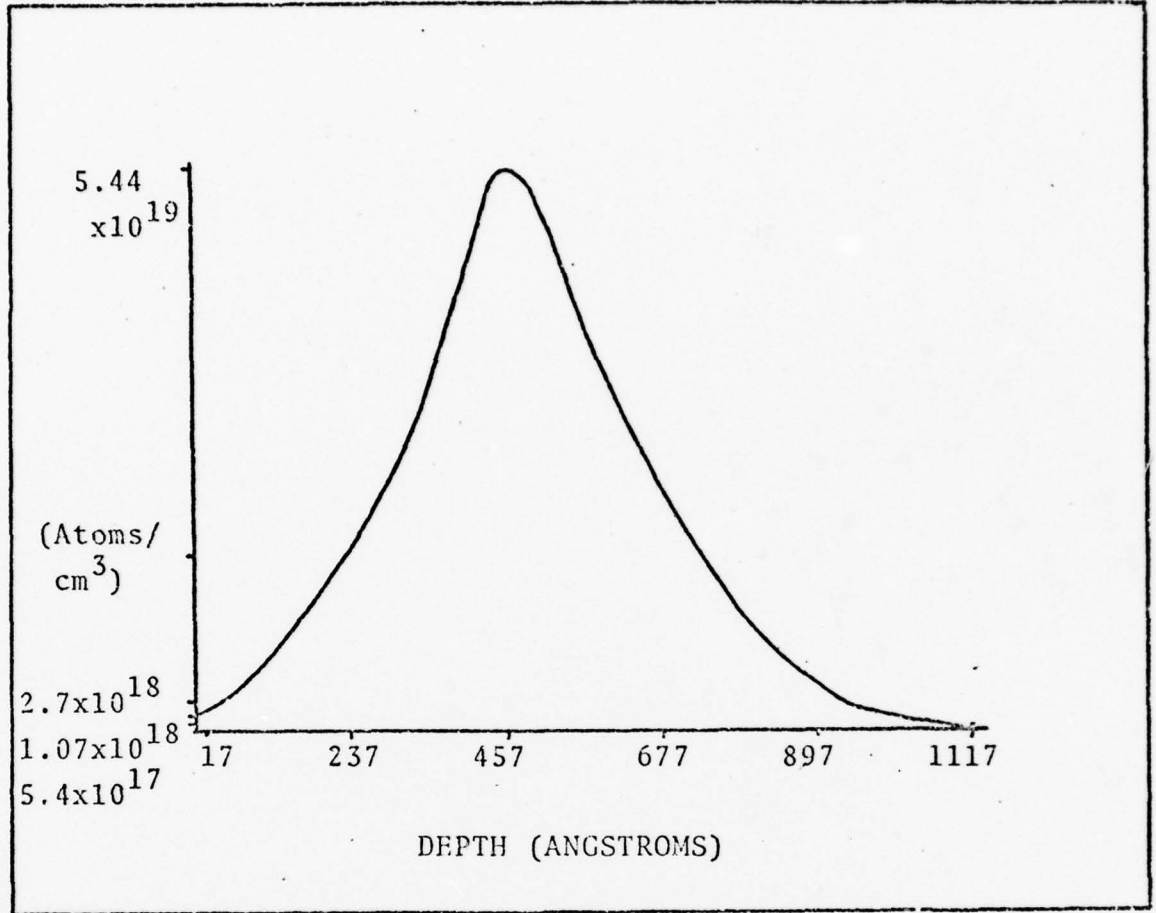


Fig 2. LSS Profile of Germanium Implanted GaAs of Fluence 3×10^{14} Ions/cm² at 120 keV

easier to obtain an ion beam of a particular impurity element than it is to find a diffusion source for that element.

The immediate result of the implant process is that it usually creates a thin layer of material at or near the surface of the crystal. The impurity atoms have penetrated the substrate and are at rest inside it, but they have not been activated nor have the damage effects of all the displaced substrate atoms, which result from an implantation step, been

healed.

For conditions of practical importance in implantation, the radiation damage produced by the injected ions is severe, and the crystal must be carefully annealed if the electrical effects of the implanted ions are to dominate the residual damage (Ref 19:1083). Gibbons outlines the basic defects as those caused by vacancies--interstitial pairs (Frenkel defects), vacancies-impurity pairs, divacancies, dislocation lines and loops, and vacancies with interstitial platelets (Ref 19:1064). Studies have been made on GaAs that clearly indicate that the degree of lattice disorder depends directly on the implant dose (Ref 7:279). Some of these crystal defects can cause luminescence. Luminescence centers are produced when the defects introduce electronic states within the band gap. Some are so near the center of the band gap that they remain unionized even at room temperature and act as recombination centers for free electrons and holes (Ref 13). Once the implant process is complete, residual damage exists in the crystal. This is where annealing enters the picture.

After the GaAs sample has been ion implanted, it must be annealed to remove the radiation damaged layers. This was accomplished in this study by two methods: thermal annealing and laser annealing. In the following section, laser annealing is described, previous works are presented, and appropriate theory is reviewed.

Laser Annealing

Laser annealing is a relatively new approach to the field

of crystal annealing. It consists of irradiating an ion implanted sample with a single, short pulse of intense laser radiation. Only recently has it been shown by several workers that laser radiation can be successfully used to anneal the ion implanted regions of GaAs (Ref 4: 21: 27: 28: 40). This unique method offers new advantages over the more conventional method of thermal annealing.

First, annealing time is greatly accelerated. After ion implantation, the thermal annealing of samples is usually carried out at 600-1000°C for a specified period, such as 15-30 minutes. The shorter anneal times possible with laser annealing are thought to be due to a reduction in the activation energy of defect migration because of ionization (Ref 28:946).

A second advantage of laser annealing is that radiation defects in implanted layers can be annealed without heating the bulk sample. Young and co-workers (Ref 58:139) have found that the effects of laser annealing can be confined to the damage region by the proper choice of wavelength and energy density.

The third important advantage deals with the temperature of the anneal. By employing a focused light beam, local annealing at different temperatures at various parts of the sample is possible.

Not only is the irradiation accompanied by heating, but because pulsed laser irradiation is characterized by a time constant of 10^{-3} (single pulse) to 10^{-11} seconds, it is accompanied also by ionization, shock waves, and quenching. These

factors affect the removal of unwanted defects and their interaction with impurities (Ref 29:445). Young and co-workers (Ref 57:139) observed that in laser annealed silicon samples there was substantially less residual damage than in the thermally annealed samples.

To induce the transition of an amorphous region into a single crystal, the correct threshold laser energy density must be found, assuming one exists. Rimini, et al. (Ref 42:154) accomplished this by laser annealing several silicon samples to establish boundaries within which was located the correct energy density value. This threshold energy density is dependent on the thickness of the amorphous layer as well as the crystallographic orientation. Lower values of the energy density produce polycrystalline materials or heavily disordered crystalline regions. Higher than threshold values produce surface damage which can usually be detected using visual methods (Ref 38).

This method is the impetus for the investigative efforts in this study of the GaAs samples 5, 6, and 7 provided by Mason (Ref 38). It was hoped that a boundary about the threshold energy density could be established using both visual methods and cathodoluminescence.

Kachurin and co-workers (Ref 29:445) suggest that there will be possible surface decomposition during the laser annealing of uncapped samples. Since all laser annealed samples in this study are uncapped, this may have a direct effect on the emission spectra.

Other relevant phenomena requiring research attention exist. For example, studies show an additional absorption of light in ion implanted samples (Ref 38; 16:85). After laser annealing the implanted sample, the light transparency returned to its original value. The exact mechanism responsible for the increased absorption of light is unknown. A possibility is that this phenomenon is linked with non-radiative centers wherein energy is converted to heat within the crystal. Another idea promulgated by Coates (Ref 11:96) is that due to disordering, optical transitions between density of states' tails in the forbidden gap cause this phenomenon to emerge.

Another example of notable interest is the mechanism behind which an amorphous region of about 1000\AA (angstroms) is able to crystallize in about 10^{-7} seconds (Ref 31). Rimini and co-workers point out (Ref 42:155) that to grow a 1000\AA thick amorphous layer in 10^{-7} seconds, a growth rate of 10^{10}\AA is required. This is orders of magnitude higher than the maximum rate normally used for growing single crystals of GaAs.

In light of these considerations and the threshold energy density values found in the amorphous to single crystal transition of Si and GaAs, Rimini (Ref 42:155) makes the suggestion that, in laser annealing, the processes involved could be related more to liquid state than to solid state epitaxy. The energy deposited by the laser pulse in the absorbing layer increases the layer temperature up to the melting point, thus melting the damaged layer.

Numerous methods are used to compare laser annealed samples

with thermal annealed samples. These include surface spreading resistance measurements (two-point and four-point probes), Secondary Ion Mass Spectroscopy (SIMS), Rutherford backscattering, channeling, Transmission Electron Microscopy (TEM), and electrical analysis (Ref 34:149; 17:142). To date, no comparison studies have been published on laser annealing and thermal annealing using cathodoluminescence.

Electron Beam Penetration

Cathodoluminescence employs electron beam energy versus sample penetration depth characteristics. As the electron beam energy is increased, the penetration depth into GaAs increases. Several studies have been made to determine the penetration depths of electrons impinging on GaAs samples at an angle of 45° .

In 1973, Norris and co-workers (Ref 39:3209) used the universal stopping curve to calculate that, for electron beam energies of 5, 10, and 20 keV, the electrons penetrated to a depth of about 1400, 4800, and $16,000\text{\AA}$, respectively.

Martinelli and Wang (Ref 37:3351) developed an empirical formula by investigating electron penetration of films of various thicknesses. They determined the maximum penetration of depth of 5, 10, and 15 keV electrons to be about 2800, 7800, and $14,000\text{\AA}$, respectively.

In 1978, Cone (Ref 12) investigated the electron penetration depth of GaAs using the Monte-Carlo method. The results indicated that the maximum penetration depths of 5, 10, and

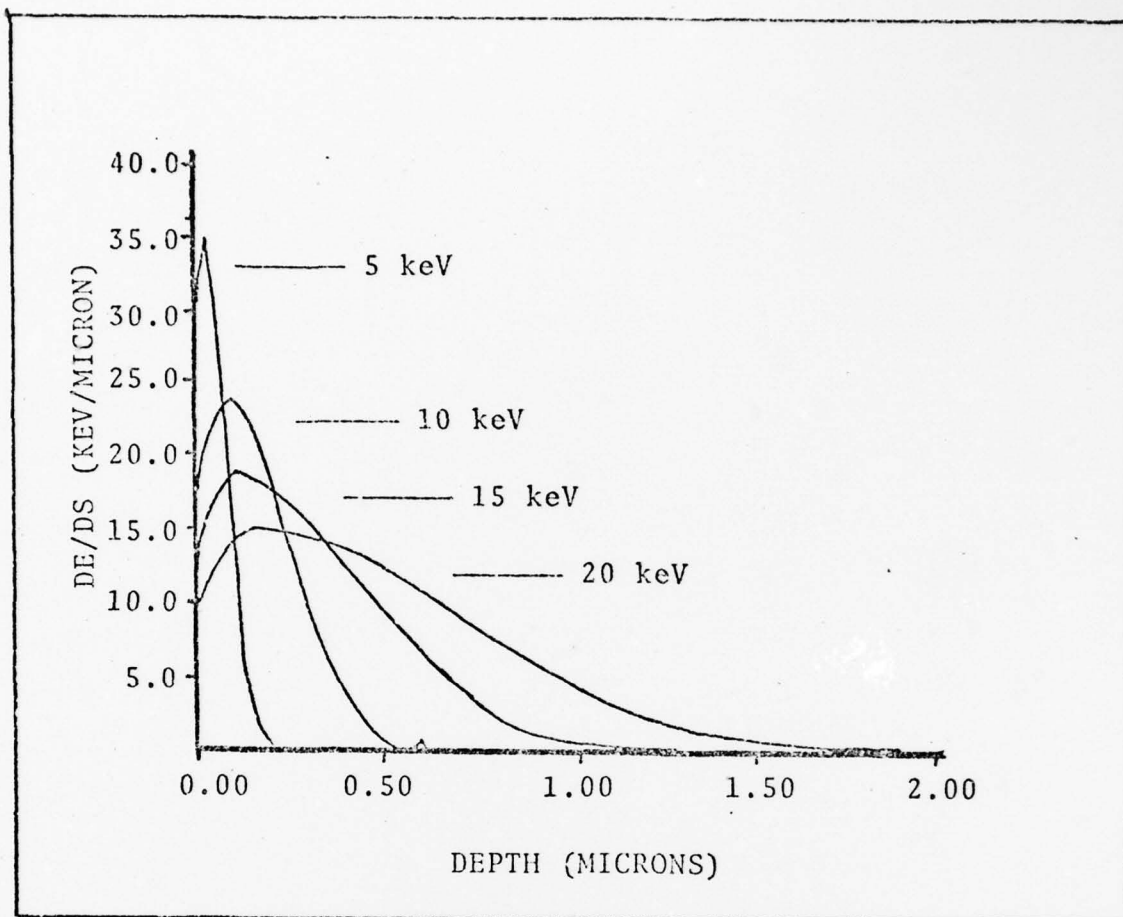


Fig 3. Estimated Electron Beam Excitation Profiles in GaAs (Ref 12)

15 keV electrons should be approximately 1900, 5000, and 11,300 \AA , respectively (see Fig 3). A summary of all three results is shown in Appendix B. It should be emphasized that the greatest amount of electron energy is lost near the surface (within 2500 \AA at 15 keV) rather than at the maximum electron penetration depth for that energy.

Impurities and Lattice Vacancy Competition

The samples used throughout the present study are known to be relatively low purity and often contain such impurities as

copper (Cu), zinc (Zn), silicon (Si), and carbon (C). These native impurities under conditions of various annealing temperatures, will compete for lattice vacancy positions. Hwang observed (Ref 25:5353) that with or without heat treatment, external sources could supply sufficient quantities of Cu to saturate the crystal. Today it is widely accepted that Cu diffuses into Cr-doped (Si) GaAs substrates such as those used in this study.

In recent studies, Ashen and co-workers (Ref 1:1051), Koschel, et al. (Ref 32:98) and Lidow, et al. (Ref 34) concluded that Zn, C, and especially Si are native impurities to most GaAs samples, including the various epilayers.

Each of the above enumerated impurities has a characteristic vapor pressure, diffusion rate, and distribution coefficient which are temperature dependent. Since this temperature dependence exists, the different impurities are thought to diffuse in and out of lattice vacancies at different rates. This is especially important when considering different annealing temperatures and annealing times. Hwang (Ref 25:5351) found for example, that during thermal annealing at $T \leq 870^{\circ}\text{C}$, Cu impurities replaced arsenide vacancies (V_{As}) given up by what is believed to be Zn (Ashen 1:1051), while Si apparently remained affixed to its V_{As} and gallium vacancies (V_{Ga}) lattice points. As the thermal annealing temperature was raised to $T \geq 900^{\circ}\text{C}$ though, both Cu and Zn yielded V_{As} vacancies to Si and the dominant peak shifted to one attributed to Si_{As} , thus converting the n-type Cr-doped (SI) GaAs substrate to p-type.

In another unrelated study, Koschel and co-workers (Ref 32:98) observed in liquid phase epitaxy (LPE) and Cr-doped (SI) GaAs at $T = 740^{\circ}\text{C}$, that C atoms transferred from Ga to As sites. Additionally, experiments on Si-doped n-type bulk GaAs demonstrated that at 800°C , Si diffused from Ga to As sites. Similar results are also reported by Lum and Wieder (Ref 35: 213).

In 1978, Lum and co-workers (Ref 36:3333) investigated Ge-doped GaAs grown by LPE methods. Ge is primarily a shallow acceptor in LPE GaAs. Since it has a lower vapor pressure than Zn, as well as a small diffusion and distribution coefficient, its impurity level was easily controlled. They concluded that thermally generated V_{As} in the vicinity of the interface were occupied by Ge atoms leading to a reduction in deep-level complexes attributed to $V_{\text{As}}\text{-C}_{\text{As}}$ and a dominating (F-B) spectral peak at 1.483 eV.

III. Experiment

The cathodoluminescence system and the procedures used in this study have been reported in previous studies (Ref 12; 52:18). For additional, detailed information these works should be consulted.

This chapter is divided into the following main areas: the cooling system, vacuum system, electron gun, luminescence detection, data display, sample description, and experimental error. For a schematic of the cathodoluminescence system, see Fig. 4.

Cooling System

The cooling system was provided by an Air Products and Chemical, Inc. liquid Heli-Trans Cooler system. This system provided an optimum temperature at which cathodoluminescence spectra induced the greatest amount of information from electron-hole recombination mechanisms without harming the crystal sample being investigated. All measurements of spectra were made with this system cooled down by liquid helium to temperatures in the 10° K region.

Vacuum System

The vacuum system provided pressures down to 10^{-7} Torr in the sample chamber. This pressure was provided by a mechanical pump and two diffusion pumps with a Union Carbide

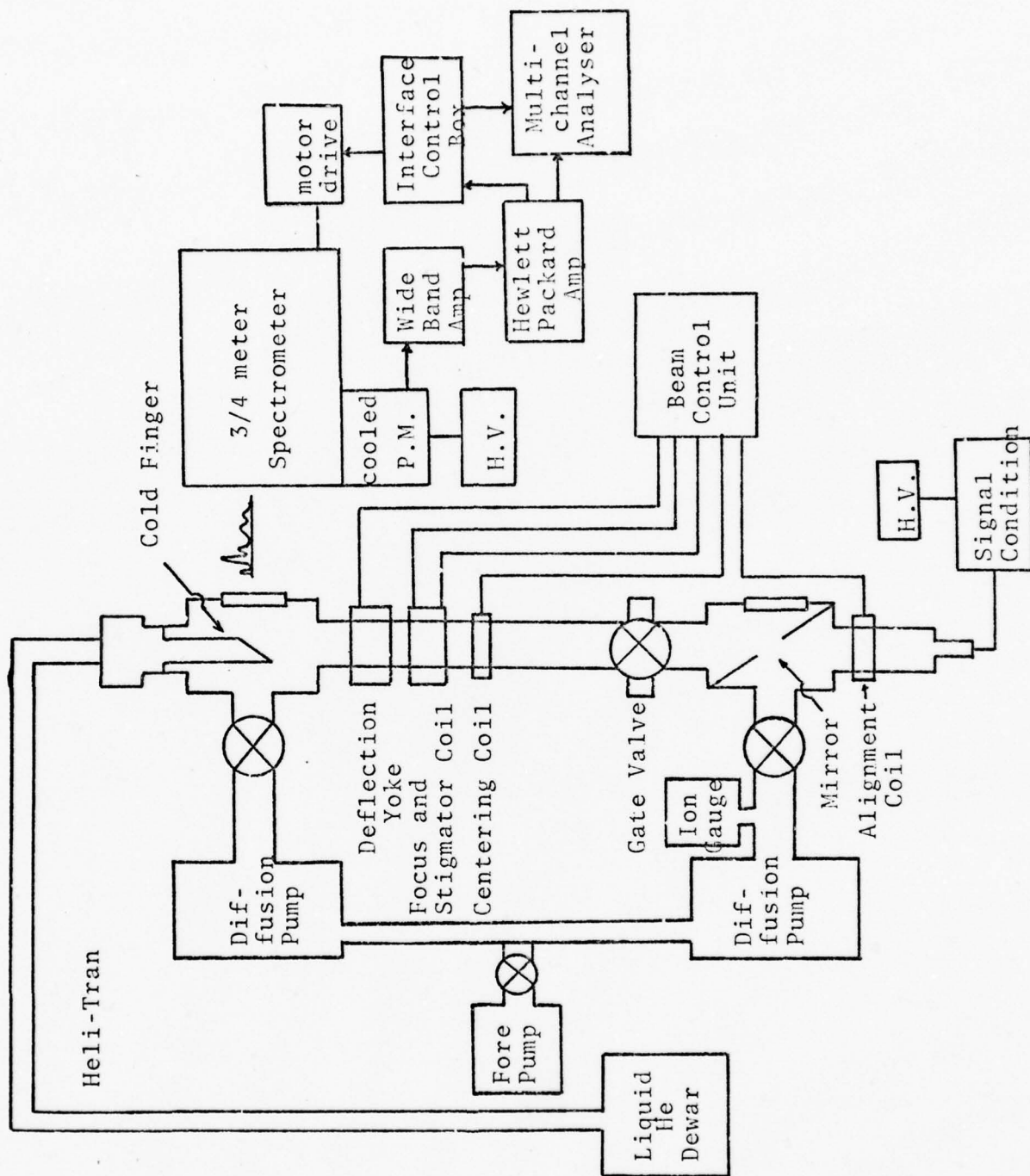


Fig. 4 Schematic of Cathodoluminescence System
(Ref 52:19)

Nitrogen trap to act as a filter.

Electron Gun

The electron gun was of standard design and originally manufactured by Hughes Aircraft Company, Vacuum Tube Products Division. The gun cathode was operated at 5-15 keV potential with the anode at ground. This limit was placed on the electron gun since voltages higher than 15 keV were found to cause arcing in the system. In normal operation, the Grid 1 and Grid 2 potentials were operated at 0 and 200 volts, respectively.

The electron gun housing was located in a mount under the mirror block. An alignment coil was installed over the mirror block to correct for misalignment of the gun. Additionally, a centering coil, focus coil, and deflection coil were included to position the electron beam generated by the electron gun onto a 45° angle, inclined sample holder. The beam current was measured by directing the beam from the sample into a Faraday cup.

Detection System

From the sample chamber, the induced luminescence from the sample traveled through a quartz window and was focused onto the spectrometer slit by a plano convex quartz lens and two spherical quartz lenses mounted on an Ealing 50 centimeter optical bench. One convex lens has a focal length of 10 centimeters and was positioned at approximately this distance from the samples. The other two lenses of 25 cm and 6.5 cm focal length were in the same mount with a fixed separation of 8 cm,

and they were positioned near the spectrometer slit. A Spectra-coat Varipass number 650 filter of set 6193 was also placed in the mount to prevent radiation of wavelengths below 6500\AA from entering the spectrometer (Ref 5:23).

The luminescence was examined by a Spex 1702 3/4-meter Czerny-Turner spectrometer. The spectrometer was equipped with a 1200 lines/mm grating which was blazed to 5000\AA . A Spex Model 1752-3 motor drive unit and Interface/Control box, designed and constructed by G. Gergal, provided external stepping signals to the spectrometer (Ref 6:27; 15:19). An RCA C70007A photomultiplier tube, operating at 50°C with S1 response, was used to detect the radiation emission scanned by the spectrometer.

Data Display

The photomultiplier tube converted the incident radiation into electrical pulses which were then processed by a Model 1121 Princeton Applied Research Amplifier Discriminator and Discriminator Control Unit. The signal was then amplified by a Hewlett-Packard amplifier. From the Hewlett-Packard amplifier, the signal was passed to a Hewlett-Packard Model 5400 multi-channel analyzer (1024 channels) for counting.

Sample Description

In this experiment 10 samples were investigated using various electron beam energies. Samples 1, 2, 3, and 4 (Group #1) were intended to provide a basis from which laser annealed samples could be properly interpreted using comparison

TABLE I
Sample Description

Group	Sample	Control Code	Type Anneal ¹	Fluence/ Type Implant ² (ions/cm ²)	Implant Temp ²	Implant Energy (keV)	Anneal ³ Energy Density (j/cm ²)
#1	1	48	U.A.	none	--	--	--
	2	47	U.A.	3E14/Ge	RT	120	--
	3 ⁴	39	T.A.	3E13/Ge	RT	120	--
	4 ⁴	40	T.A.	3E14/Ge	RT		--
#2	5	51	L.A.	None	--	--	> .24
	6	49	L.A.	None	--	--	≅ .24
	7	50	L.A.	None	--	--	>> .24
#3	8	42	L.A.	3E14/Ge	RT	120	.24
	9	43	L.A.	3E13/Ge	RT	120	.252
	10	41	L.A.	3E13/Ge	RT	120	.24

¹U.A. = Unannealed; T.A. = Thermal Annealed; L.A. = Laser Annealed

²RT = Room Temperature

³Calibrated Laser Annealed Density Values (Ref 38)

⁴These samples were annealed at 850°C for 15 minutes

techniques. Samples 5, 6, and 7 (Group #2) were examined to provide threshold density information in addition to laser annealed spectra information. Finally, Samples 8, 9, and 10 (Group #3) provided the core of the investigative efforts.

Table I provides a summary of specific sample information. All samples are characterized by Cr-doped, semi-insulating (SI), as-grown GaAs substrates. Samples 3 and 4 have 1000Å

Si_3N_4 caps, while all other samples are uncapped.

All the samples investigated were provided by the Air Force Avionics Laboratory, Wright-Patterson AFB, Ohio. Samples 5-10 were laser annealed by Mason in a concurrent study (Ref 38). His work should be consulted for a more comprehensive look at the methods used.

Experimental Error

To determine the degree of experimental error, the following error analysis was performed. From

$$\lambda = [(x \pm n) - (y \pm n)]L + \lambda_c \quad (6)$$

where

λ = wavelength of spectrum data point

x = channel number of data point

y = channel number of calibration line peak

n = possible error in MCA = ± 1 channel

$L = \frac{\text{wavelength region investigated}}{\text{number of channels used in MCA}} = \frac{1777.8}{1024} = 1.73611$

$\lambda_c = 8014.8\text{\AA}$ (calibration line wavelength)

Substituting in the above applicable information yields

$$\lambda = [(x \pm 1) - (y \pm 1)]1.73611 + 8014.8\text{\AA}$$

Case I. Peaks in the first half of MCA (for example, $x = 186, y = 7$)

$$\lambda = [(186 \pm 1) - (7 \pm 1)]1.73611 + 8014.8\text{\AA}$$

$$\lambda = [179 \pm 2]1.73611 + 8014.8\text{\AA}$$

$$\lambda_1 = 8322.0914\text{\AA} \quad (\text{for } -2)$$

$$\lambda_2 = 8329.0359\text{\AA} \quad (\text{for } +2)$$

Therefore, since $E_p = \frac{12398.54}{\lambda}$ (ev) where E_p is the spectral peak energy, a maximum possible error of 1.24 meV exists for this case.

Case II. Peaks in the second half of the MCA (for example, $x = 652$ and $y = 7$)

$$\lambda = [(652 \pm 1) - (7 \pm 1)]1.73611 + 8014.8\text{\AA}$$

$$\lambda = [645 \pm 2]1.73611 + 8014.8\text{\AA}$$

$$\lambda_1 = 9131.1187\text{\AA} \quad (\text{for } -2)$$

$$\lambda_2 = 9138.0631\text{\AA} \quad (\text{for } +2)$$

Therefore, a maximum possible error of 1.03 meV exists for this case. Hence, these results indicate that recorded emission spectra are accurate to within approximately ± 1 meV.

IV. Results and Discussion

The data presented in this chapter was obtained from ten samples. These samples, described individually in the previous chapter, are divided into three areas labeled Group #1, Group #2, and Group #3. The Group #1 samples represent the basis group which, through comparison with the other two groups, will yield more informative observations. Group #2 represents unimplanted samples examined in an effort to establish the threshold energy density for laser damage in low purity Cr-doped (SI) GaAs. Finally, Group #3 contains the laser annealed ion implanted (Ge) samples. As noted in Chapter II, the samples used throughout the present study were Cr-doped, semi-insulating crystals of GaAs. Such crystals are known to be of relatively low purity and to often contain such impurities as copper (Cu), zinc (Zn), silicon (Si), and carbon (C). Further, under various annealing temperatures, annealing times, and quenching times, the different native impurities will compete for lattice vacancy positions induced by the annealing process. In addition, the various fluences of the added implant element induce damage defects by the implantation process. Therefore, the emission spectra of unannealed, thermally annealed, and laser annealed samples must be interpreted by considering all of these factors.

Cathodoluminescence of Group #1

Group #1 is composed of Samples 1, 2, 3, and 4. Samples 1

and 2 are the unannealed unimplanted, and unannealed 3×10^{14} ions/cm² Ge implanted samples, respectively. Samples 3 and 4 are the thermally annealed Ge implanted samples of fluences 3×10^{13} ions/cm² and 3×10^{14} ions/cm², respectively. The CL results of each of these samples, described in Chapter III, will be discussed individually (see Table I).

Sample 1. A typical spectrum for Sample 1 at 10°K, obtained with an electron beam energy of 10 keV, is shown in Fig 5(a). The near band edge peak located at 1.515 eV is attributed to unresolved exciton recombinations (Ref 23; 45; 55). The spectrum indicates additional peaks at 1.492, 1.48, 1.471, 1.407, and 1.36 eV. From past studies, these are attributed, respectively, to (F-B) C_{As}, (F-B) Ge_{As} from trace elements, V_{As} related defects, V_{As}-acceptor complexes, and a weak peak due to Cu_{Ga} (Ref 1:1051; 9:1421; 26:4; 47:423). The dominant peak appears to be due to the native impurity carbon. As can be seen from Appendix B, this emission excited with 10 keV electrons is characteristic of luminescence from the surface to a maximum depth of about 5400Å.

Sample 2. This sample was probed at 10°K using electron beam energies of 5, 10, and 15 keV. Typical emission spectra (see Fig 5(b)) indicated surface damage at the 5 keV range. At 10 keV (maximum depth of about 5400Å), the luminescence was characteristic of the native impurities C (1.494 eV) and Zn (1.49 eV); also observed here were peaks at 1.515, 1.469, 1.4 and 1.36 eV (see Fig 5(c)). Luminescence at 15 keV (a maximum depth of about 1.1 μm), shown in Fig 5(d), essentially indic

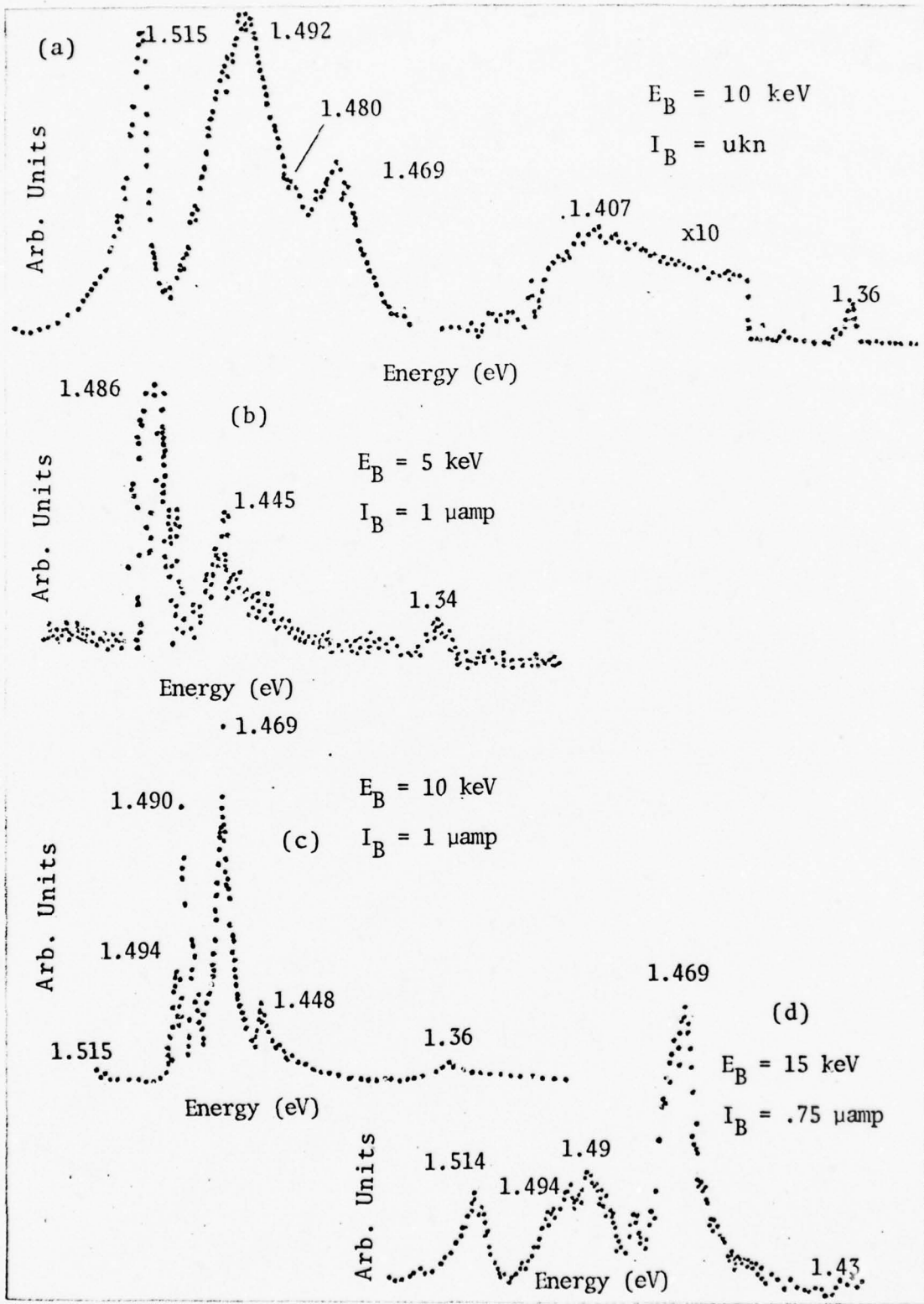


Fig 5. The CL Spectra Obtained at 10°K on Sample 1 (a) and Sample 2 (b-d)

the same observed peaks with the difference being the latter spectra were much lower in intensity. Since the implant depth is about 1000\AA , these results seem to support the contention that the spectral results are characteristic of native impurities, and that the Ge implanted atoms are on non-radiative sites. At 15 keV, the observed peak at 1.477 eV is attributed to Ge. As was noted in Sample 1, the 1.47 eV peak attributed to V_{As} related defects was also observed in this sample. It should also be noted that at 10 keV only, a 1.36 peak attributed to Cu_{As} was observed (Ref 25:5331; 54:254; 57:271). Furthermore, the 1.40 eV V_{As} -acceptor complex peak and the 1.37 eV V_{Ga} defect related peaks were not observed in this sample. At 10 keV, the 1.49 eV (Zn) and 1.47 eV (V_{As} defects) peaks were nearly equal in dominance, while at 15 keV, the 1.47 eV band was the predominant peak.

Sample 3. Typical spectra for Sample 3 at 10°K for the different excitation energies of 5-15 keV are shown in Figs 6 and 7. At 5 keV, the dominant peak was the 1.398 eV band. As the excitation energy was increased to 7.5 keV, the 1.398 eV peak became less dominant in comparison to the 1.36 eV band until finally at 15 keV, the 1.36 eV band dominated the 1.398 eV band.

The literature indicates that the 1.398 eV band is associated with V_{As} -acceptor complexes (Ref 8:144). This present data tends to support this contention. As one probes deeper into the sample, the relative intensity of the 1.398 eV band compared to the 1.36 eV band significantly decreases in

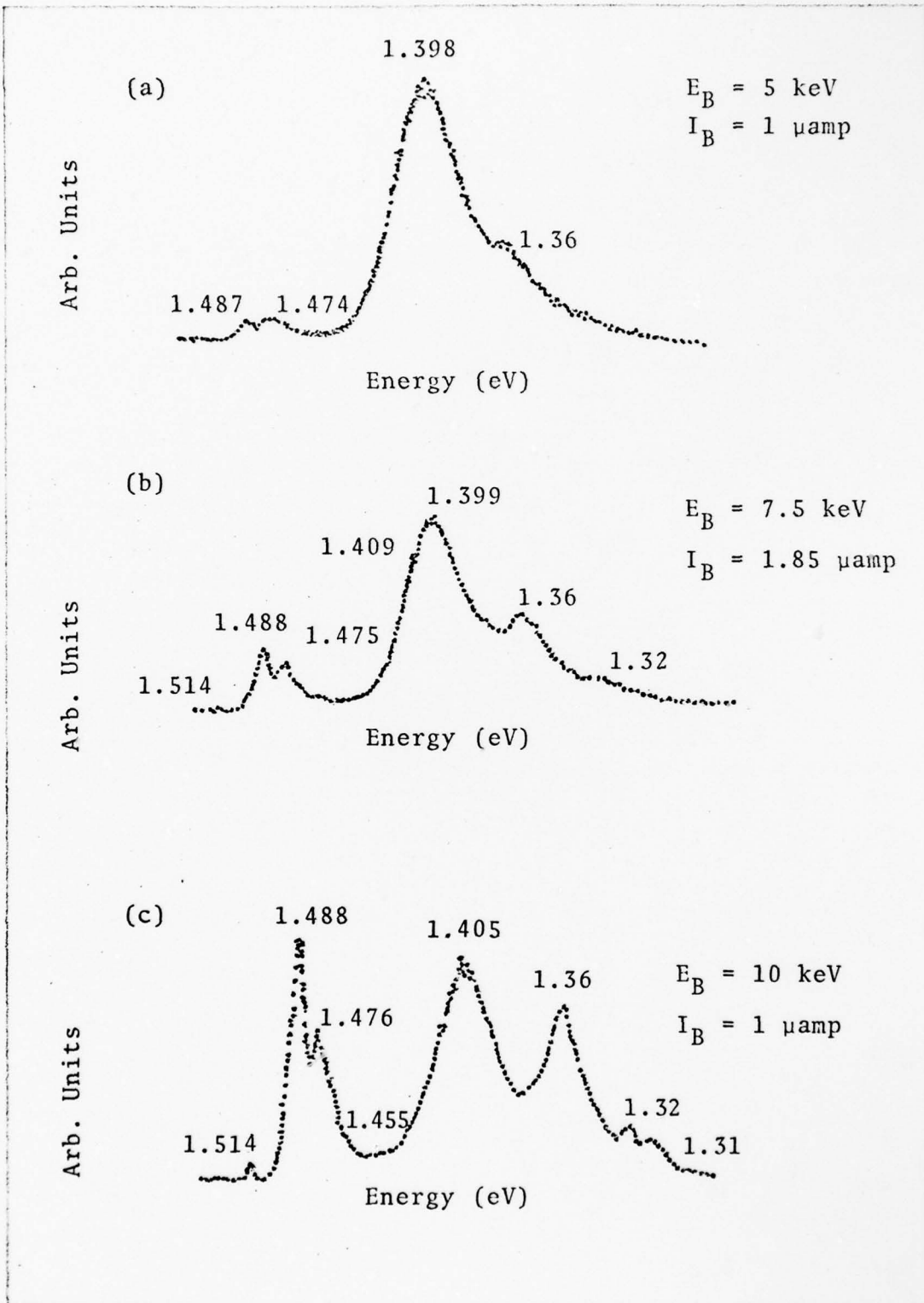


Fig 6. The CL Spectra Obtained at 10°K on Sample 3 at 5, 7.5, and 10 keV

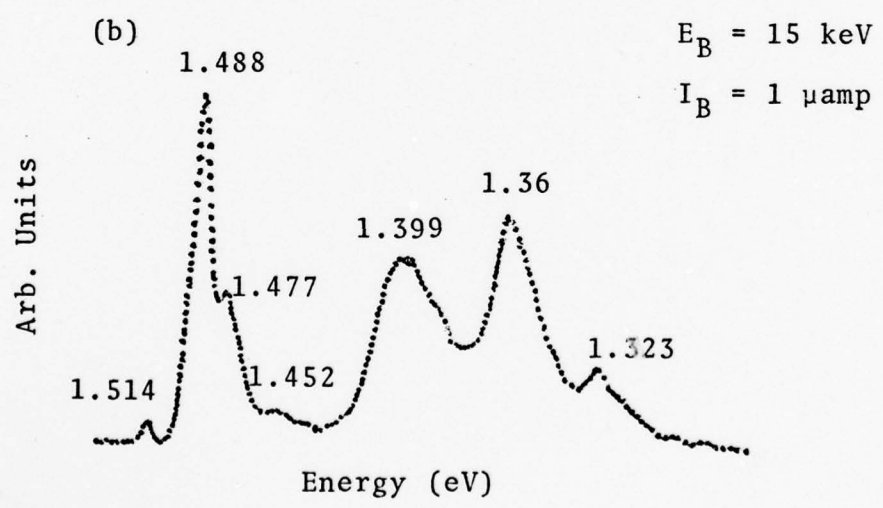
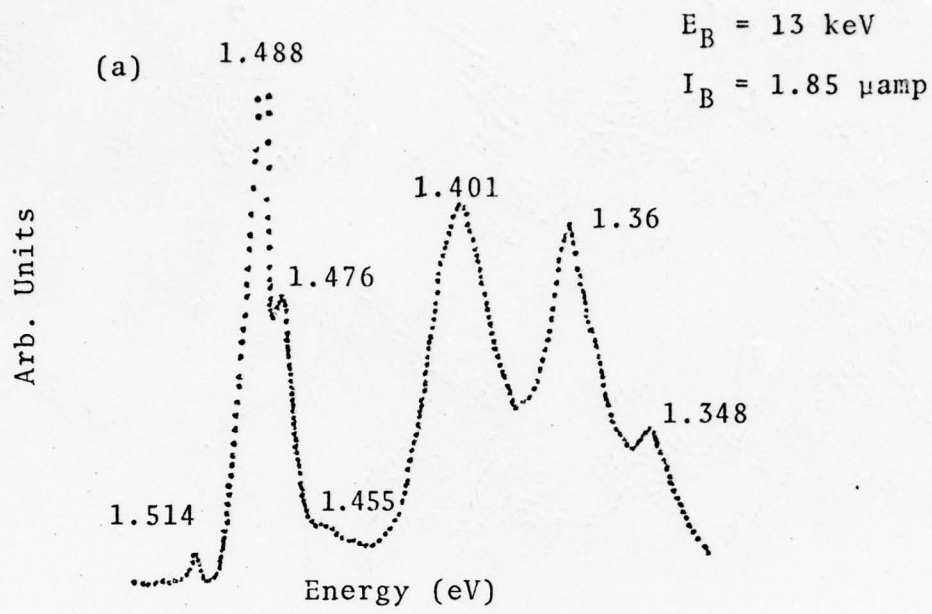


Fig 7. The CL Spectra Obtained at 10°K on Sample 3 at 13 and 15 keV

agreement with the above contention that arsenide diffuses outward leaving arsenide vacancies behind (Ref 9:1422).

Since the Cu impurity is assumed to be present in this sample as a native impurity, the Cu peak (1.36 eV) was chosen to normalize all other peaks. The literature indicates that the 1.36 eV band is due to a Cu impurity migrating onto gallium vacancies (Ref 54:253). Chang and co-workers (Ref 8:145), however, contend that this band is due to V_{Ga} , while a 1.37 eV band is due to Cu_{Ga} . Since these are within the limits of the experimental error of this experiment, the 1.36 eV will be referred to as an unresolved V_{Ga} defect and Cu_{Ga} band when there is doubt one way or the other. In different situations, such as SiO_2 or Si_3N_4 capped samples versus uncapped samples, one seems to be favored over the other, thus reducing the significance of the controversy in the literature (Ref 10:317).

At 5 keV, the 1.487 eV and 1.474 eV bands are totally dominated by the V_{As} -acceptor complex related band (1.398 eV) and the Cu_{Ga} (1.36 eV) band. (In this case, the 1.36 eV band is designated as a Cu_{Ga} since it is consistently strong at all depths.) At 7.5 keV, the 1.488 eV and 1.475 eV bands increase in intensity with the 1.488 eV peak the dominant of the two. At 10 keV, the 1.488 eV peak exceeds the intensity level of the V_{As} -acceptor complex related peak, while the 1.478 eV peak remains at half the intensity of the 1.488 eV band. Luminescence from 13 keV electrons indicates the 1.488 eV band has increased in intensity, while the 1.476 eV band remained at the same intensity relative to the 1.398 eV band. At 15 keV,

the 1.488 eV band increased still more in intensity compared to the 1.398 eV band, while the 1.477 eV level remained essentially at the same relative position noted in the 10 keV and 13 keV probes.

The 1.488 eV band appears to increase in intensity as one probes deeper into the crystal. Ashen, et al. (Ref 1:1051) assign a peak at 1.488 eV to a (F-B) transition with a Zn acceptor. Since the samples probed in this experiment are of lower purity than those investigated by Ashen, one might expect to find Zn at a lower energy as a result of band tailing. Although this sample is capped, Zn still out-diffuses since the densities of the cap and sample are nearly the same. This supports the observation of an increasing 1.488 eV level as one probes deeper. This idea applies also to the 1.398 eV band since As is known to diffuse outward if the sample is not SiO₂ capped or under As pressure during thermal annealing (Ref 51: 54). Figure 7 shows that at the different excitation energies, the position of the 1.488 eV peak remains constant. This seems to indicate the existence of an unintentionally doped impurity in the sample. For these reasons, then, it appears that the 1.488 eV peak is due to residual Zn impurities found in the GaAs substrate.

Ashen, et al. (Ref 1:1051) identify the Ge (F-B) peak at 1.479 eV. Because the energy is expected to be shifted to a lower value in a low purity sample, the 1.475 eV peak observed in the spectra is attributed to Ge_{As}. Figure 7 shows the fact that as the excitation energy increased, the 1.475 band

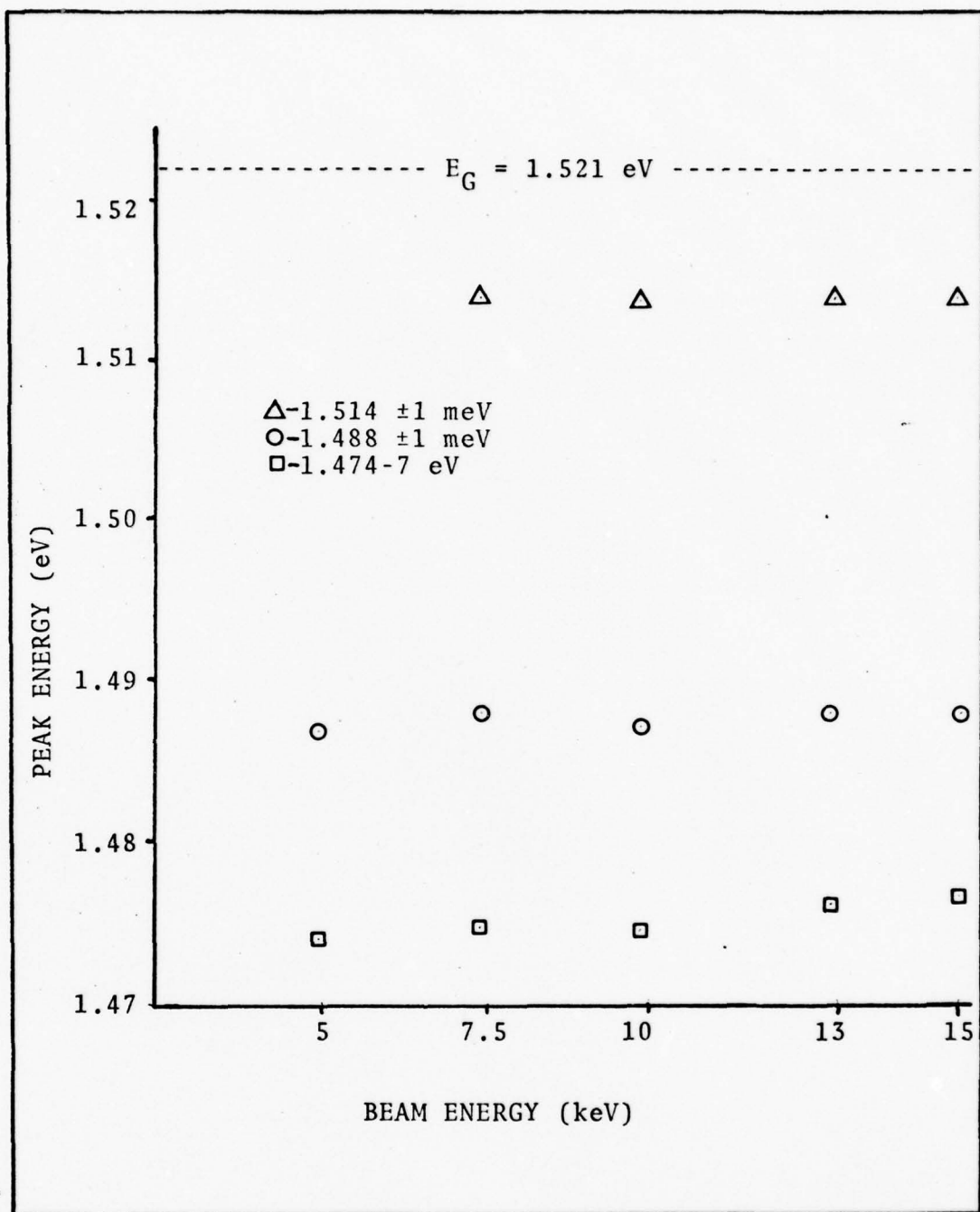


Fig. 8 Peak Energy Versus Electron Beam Energy for Sample 3

shifted (increased) about 3 meV in energy. From Eq (3), using a value of $E_D = 6$ meV (Ref 46:2225) and $E_A = 38$ meV (Ref 43:263), the spectral emission for a (D-A) is 1.475 eV. Schairer identifies the 1.478 band as a possible LO phonon replica of the 1.514 eV exciton related band (Ref 47:423). Throughout all the measurements, the 1.514 eV band has been present. Based on the intensity levels of the 1.514 band versus the 1.478 eV bands, however, one discounts the possibility of the phonon replica contention.

Sample 4. This sample was investigated using electron beam energies of 5, 10, and 15 keV (see Figs 9 and 10). These correspond to maximum depths of penetration of approximately 1900Å, 5400Å, and 1.1 μm , respectively. Since this sample has a 1000Å Si_3N_4 cap, the actual substrate penetration depths are estimated to be 900Å, 4400Å, and 1 μm (Ref 12).

At 5 keV, the 1.515, 1.492, 1.489, 1.474, 1.445, 1.403, 1.36 and 1.322 eV bands were observed. As the excitation energy increased to 10 keV, the 1.515 eV and 1.489 eV band intensities increased significantly above those of the previously observed peaks. At 15 keV, the 1.489 eV peak dominated all other peaks.

Evaluation of the simple center peaks shown in Fig 11 produced similar information as that found in Sample 3. The 1.515 eV was constant throughout the investigations at different excitation energies. This peak is, of course, attributed to an unresolved exciton complex. Within the limits of the experimental error, this peak could be due to free excitons or excitons bound to neutral donors (Ref 23:464). The 1.491 eV

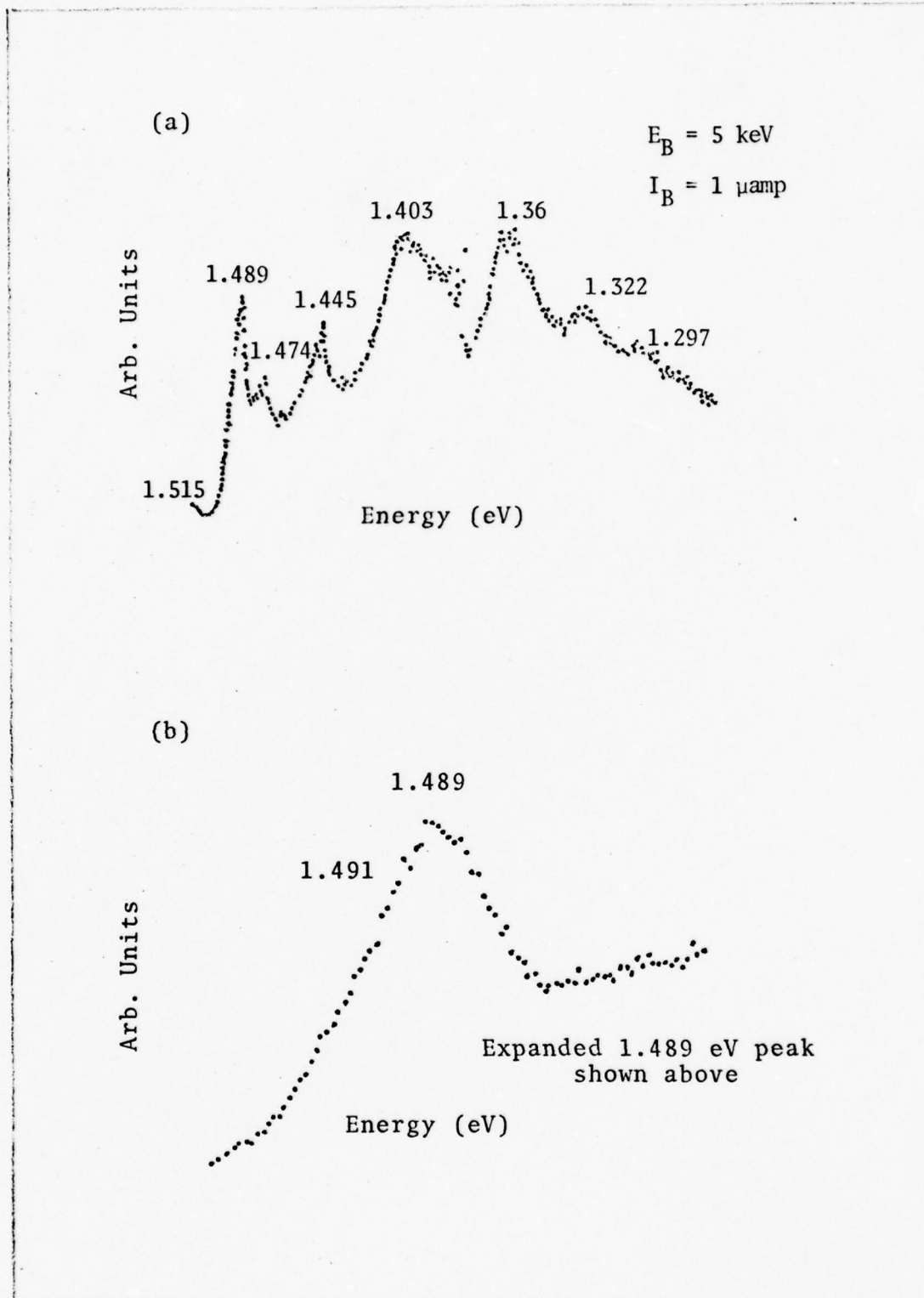


Fig 9. The CL Spectra Obtained at 10°K on Sample 4 at 5 keV

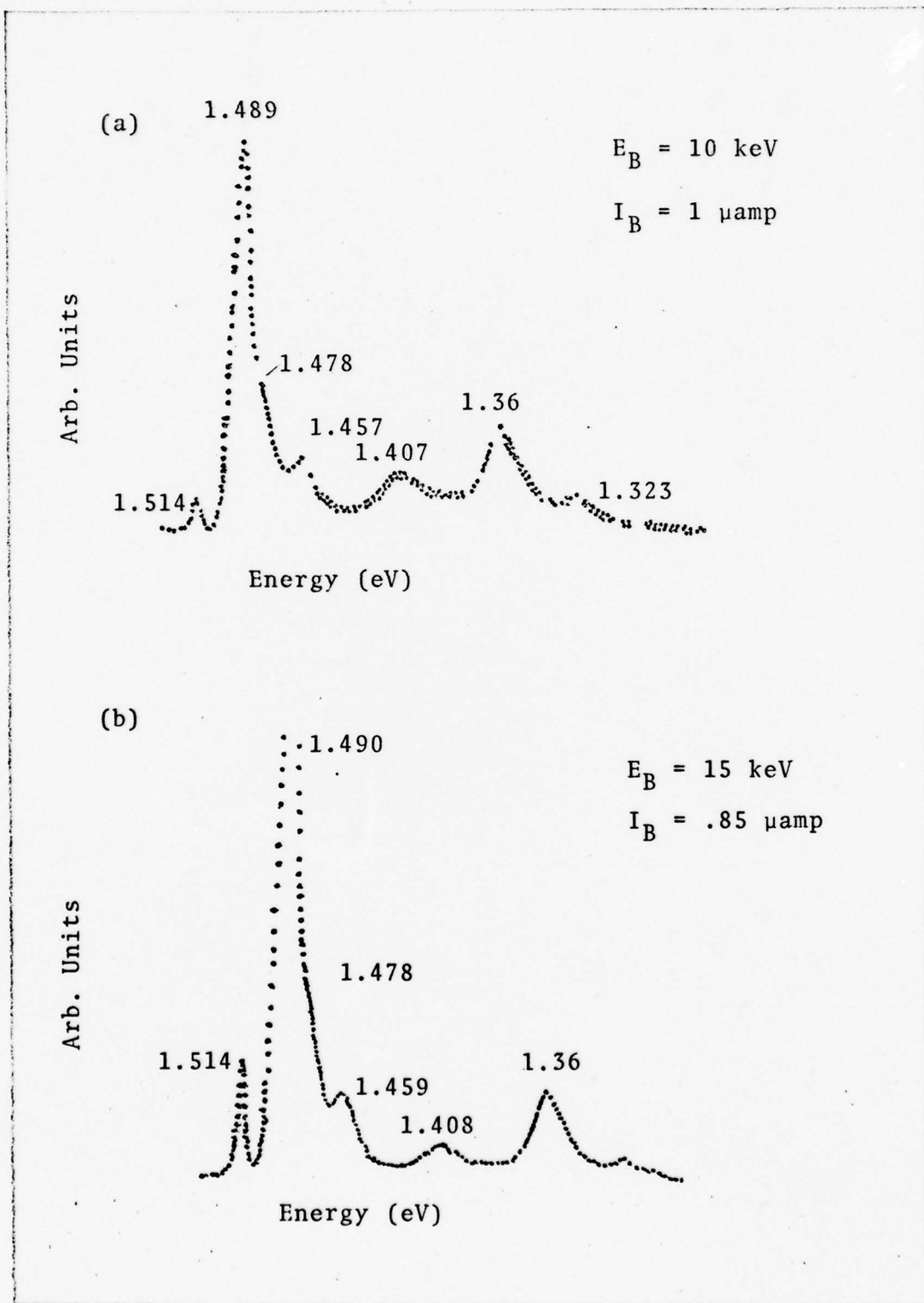


Fig 10. The CL Spectra Obtained at 10°K on Sample 4 at 10 and 15 keV

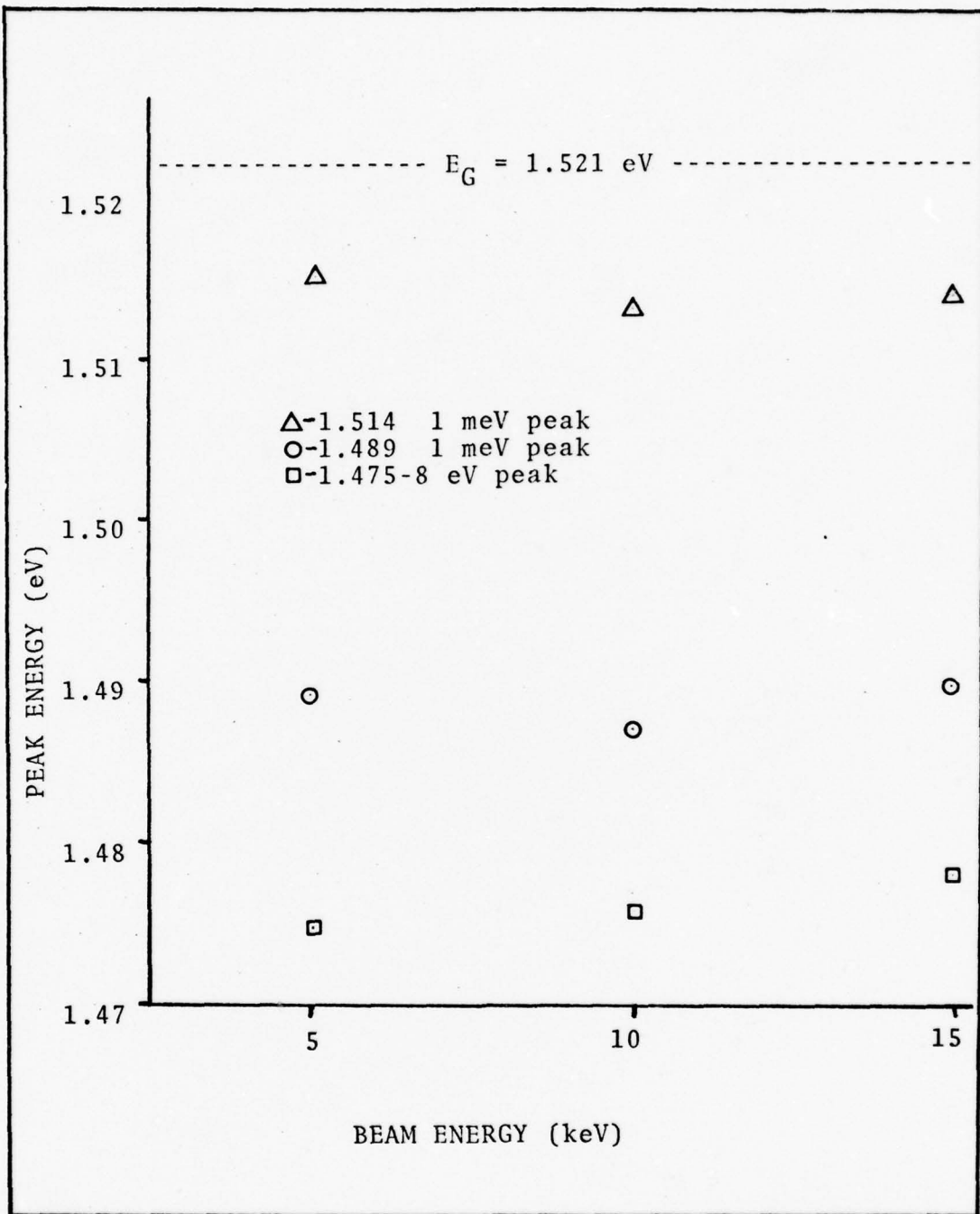


Fig. 11 Peak Energy Versus Electron Beam Energy for Sample 4

shoulder observed at 5 keV, shown in Fig 9(b), is attributed to C_{As} (Ref 1:1051). The 1.475 eV, noted in Sample 3, is again observed in these spectra. It is attributed to a possible Ge donor band-Ge acceptor band recombination. One should note that in Fig 9, again the 1.475 eV band was observed to increase in energy about 3 meV over an excitation energy range of 5-15 keV.

The 1.459 eV band is thought to be a LO phonon from an unresolved 1.494 eV carbon acceptor recombination. This claim is based on the observed low intensity of the 1.459 eV peak. In addition, the 1.491 eV peak seems to indicate the presence of C_{As} .

The 1.403-8 eV band indicates a distinct increasing shift with increasing excitation energies. This peak is generally considered to be due to V_{As} -acceptor complexes. The acceptor is possibly Ge since it is the primary dopant. Koschel and co-workers attributed $C_{As}-V_{As}$ to the 1.413 eV, while $Si_{As}-V_{As}$ corresponds to the 1.409 (Ref 32:99). Therefore, it is possible that the 1.403-8 corresponds to $Ge_{As}-V_{As}$, but more research is required to harden this plausibility argument. At 5 keV, the 1.40 eV and 1.36 eV peaks are of equal intensities. As the penetration depth is increased, the 1.40 eV band decreases while the 1.36 eV band remains essentially constant. This clearly supports the claim that the 1.40 eV is attributed to V_{As} -acceptor complexes, possible Ge as noted above. The 1.36 eV is attributed to Cu_{Ga} . Since the Si_3N_4 cap serves the purpose of containing gallium atoms, spectral characteristics

associated with gallium vacancies are not to be expected (Ref 9: 1421).

The origin of the 1.445 eV peak is not certain at this time. However, at 20°K a new Ge line was identified at 1.454 eV in Ge doped Ga_{As} by Williams and Elliot (Ref 55:1657). This line was attributed to V_{As}-Ge_{As} complexes and may account for the 1.457 eV observed at 10 keV and 15 keV. At 10°K this may explain the 1.445 eV, but more temperature variation experiments are required to substantiate this possibility. Another possibility is that a native impurity is involved on the surface layer with the V_{As}-acceptor complex causing the 1.445 eV peak. Kusano suggests in a recent study (Ref 30:4021) a diatomic donor or acceptor complex model that may explain the 1.445 eV and/or 1.471 eV in more detail. Finally, the 1.322 eV band is attributed to a LO phonon replica of the 1.36 eV Cu_{Ga} band, based on its approximate separation energy of 36 meV.

Cathodoluminescence of Group #2

Group #2 consists of samples 5, 6, and 7. These samples are all unimplanted and laser annealed at various energy density values as noted in Table I, page 25. The CL results of each of these samples will be discussed individually.

Sample 5. A typical spectrum of Sample 5 is shown in Fig 12(a). This spectrum was made at 10°K using an electron beam energy of 10 keV. A 1.515 eV band attributed to unresolved excitons, a 1.489 eV band thought to be due to Zn, and a 1.468 eV band possibly attributed to V_{As} defects were the

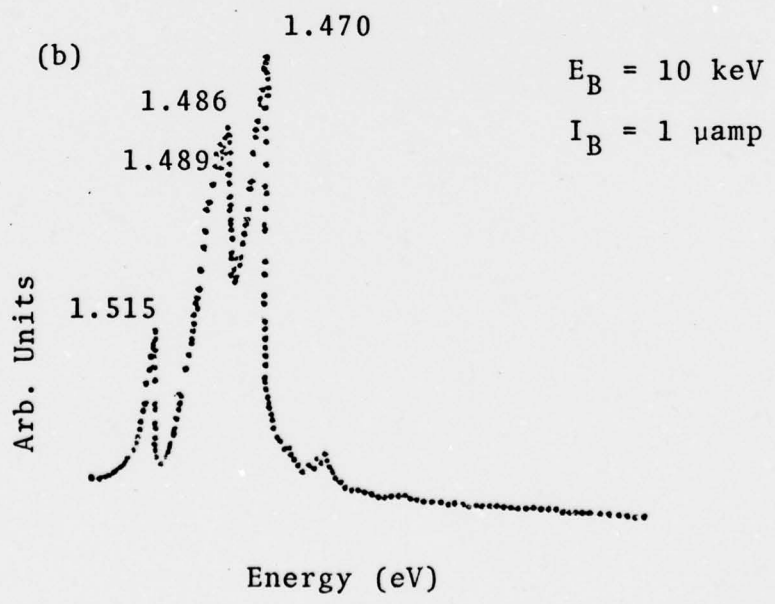
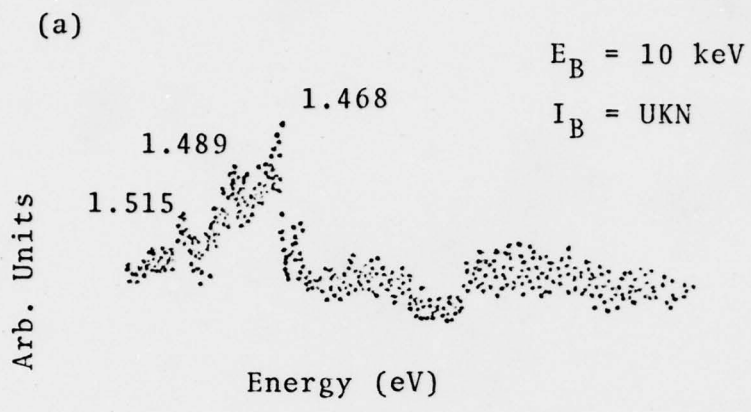


Fig 12. The CL Spectra Obtained at 10°K on (a) Sample 5 and (b) Sample 6

only spectral peaks obtained. The intensity of this spectrum was extremely low, indicating that non-radiative centers characteristic of heavy damage were dominant in this sample. The dominant peak was the 1.468 eV (damage related V_{As}) peak.

This sample has a luminescent intensity two orders of magnitude less than that obtained in Sample 1. The 1.515 eV band is observed in both spectra as is the 1.468 eV band. A distinctive difference though is the lack of a C_{As} induced band in this sample. It should also be pointed out that the lower energy peaks (below 1.468 eV) observed in Sample 1 are not observed in this sample.

Sample 6. This sample was investigated at 10°K using an electron beam of 10 keV (see Fig 12(b)). This sample was characterized by the 1.515, 1.489, 1.486, 1.470, and 1.433 eV bands. These correspond to, respectively, unresolved excitons, Zn_{As} , Si_{As} , damage related V_{As} , and a LO phonon of the 1.470 band. The spectra showed an order of magnitude more intensity than Sample 5. Again though, the 1.47 eV peak was the predominant peak. It should be noted that in this sample, the laser anneal seems to have induced Si_{As} to become an observable peak, totally dominating the Zn_{As} related peak.

Noticeable differences between this sample and Sample 1 exist. For example, the C_{As} peak which was dominant in Sample 1 is no longer observed in this sample. Additionally, the 1.470 eV peak observed in Sample 1 is the dominant peak in this sample. Finally, as was noted in Sample 5, no luminescence was observed below 1.433 eV.

Sample 7. This sample was totally non-radiative in the 1.2 eV to 1.52 eV range. At 10°K and at various excitation energies in the range 5-15 keV at 1 μ amp, no luminescence was detected.

Cathodoluminescence of Group #3

This section contains the observations of the emission spectra obtained from three laser annealed samples. These samples are Sample 8, Sample 9, and Sample 10. These will be described individually.

Sample 8. Figure 13 presents the typical spectra obtained at 10°K using electron beam energies of 5, 10, and 15 keV. The spectra obtained from the surface to about 1900Å contained the 1.447 eV and 1.36 eV peaks. Higher energy peaks were not observed in this sample at 5 keV beam energies.

The 1.447 eV is thought to be possibly related to $V_{As}-Ge_{As}$ complexes or diatomic complexes involving donors or acceptors (Ref 30:4021; 55:1657). The only basis for this contention is that it is known that this sample has been heavily implanted. If no annealing has taken place or even partial annealing has taken place, then the formation of diatomic donor or acceptor complexes from a heavy resource of interstitial Ge atoms is within the realm of possibility. It should be noted that the 1.447 eV has not been observed in unimplanted samples.

The 1.36 eV is attributed to the Cu_{Ga} band. This claim is based on several factors. First, this sample is uncapped. This allows the out-diffusion of gallium atoms to go unchecked.

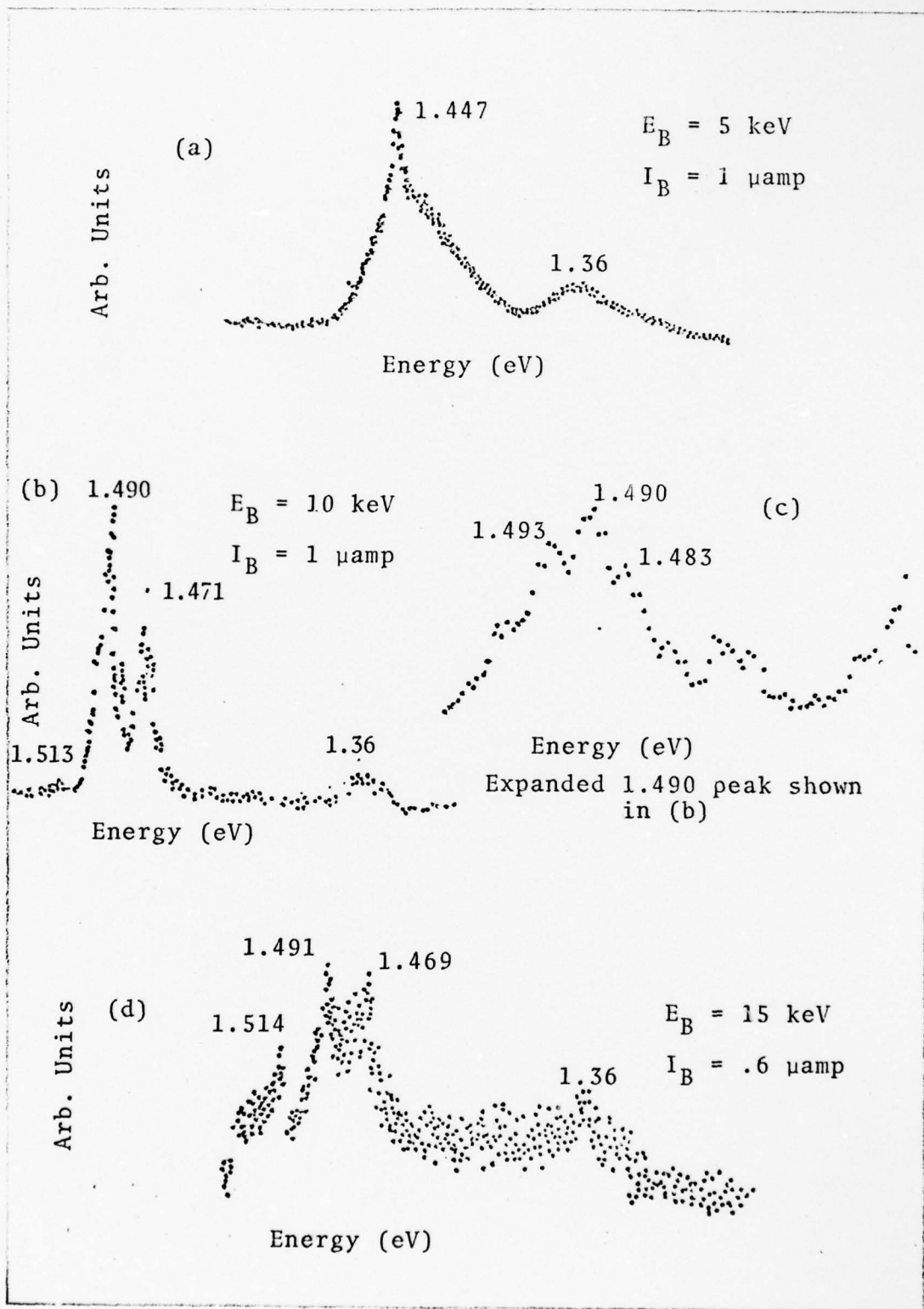


Fig 13. The CL Spectra Obtained at 10°K on Sample 8

A second factor is the presence of Cu impurities. Since Cu_{Ga} induced peaks were observed in the Si_3N_4 capped thermal annealed samples, the statement that Cu is indeed present is fully justified. Therefore, since V_{Ga} defects are expected to be low, the 1.36 eV band is attributed to Cu_{Ga} .

From the surface to a depth of about 5400\AA , the luminescence peaks observed were the 1.513, 1.493, 1.490, 1.483, 1.471, and the 1.36 eV peaks. These correspond, respectively, to unresolved excitons, C_{As} , Zn_{As} , Si_{As} , V_{As} damage (defect related), and Cu_{Ga} . These have been described in previous samples. Especially noteworthy here is the fact that this spectrum, at 10 keV, provided the same peak information as that obtained from Sample 2 at 10 keV, except that the intensity from this sample was an order of magnitude less.

At 15 keV (a maximum penetration depth of about $1.1\ \mu\text{m}$), the intensity dropped again by nearly an order of magnitude. In this spectrum, the 1.514, 1.491, 1.469, and 1.36 eV peaks were observed. These have been previously described. Again this extremely low intensity count seems to indicate severe damage since there is an excessive number of non-radiative centers.

Sample 9. Typical spectra of Sample 9, measured at 10°K , produced by 5, 10, and 15 keV electron beam energies are shown in Fig 14. The significant surface layer peaks obtained at 5 keV were 1.480, 1.455, 1.448, and 1.36 eV.

The 1.480 eV band is attributed to Ge_{As} (Ref 1:1051). The 1.455 eV and 1.448 eV peaks have been previously attributed

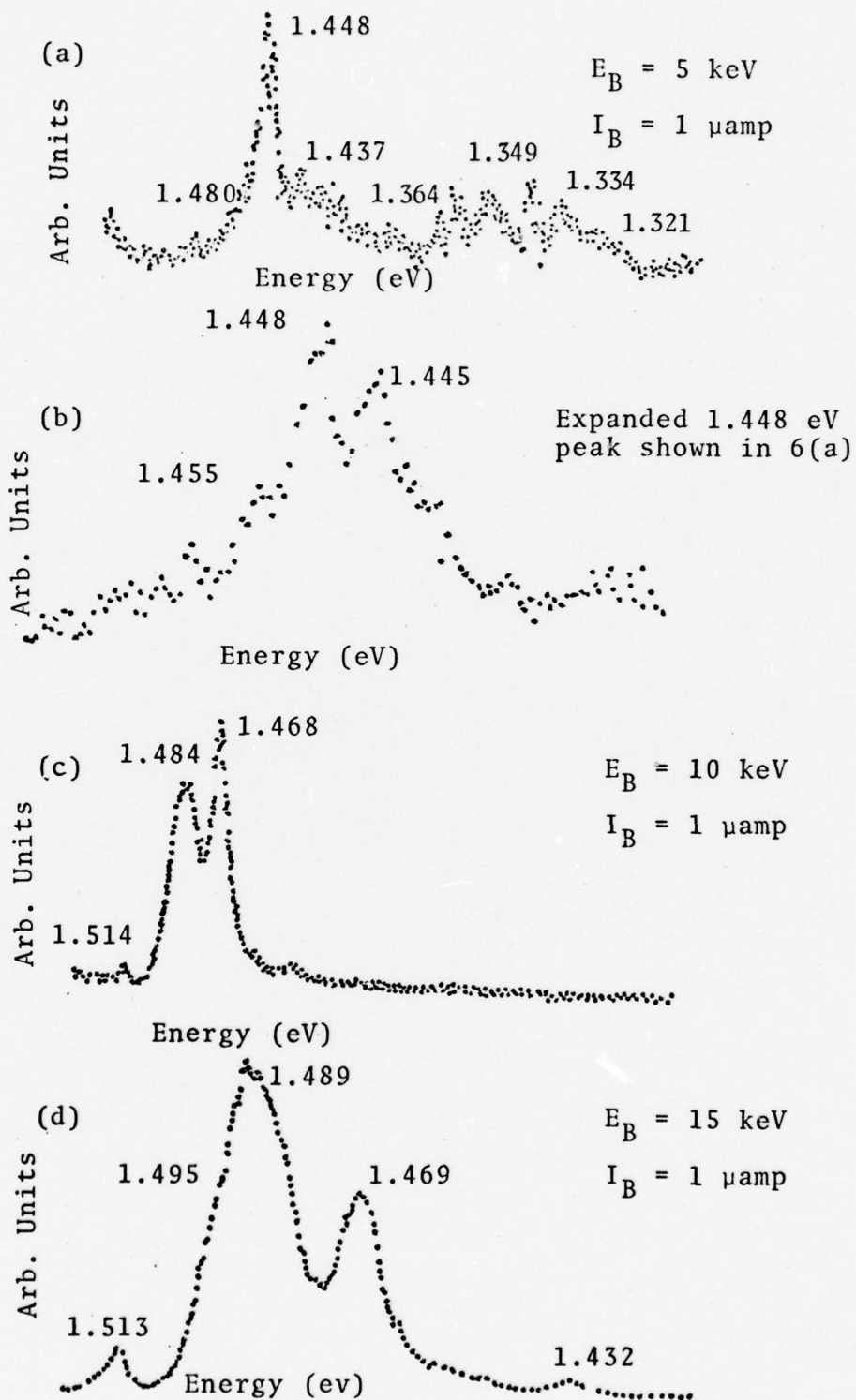


Fig 14. The CL Spectra Obtained at 10°K on Sample 9

to possible $V_{As}-Ge_{As}$ complexes and diatomic complexes, respectively. The 1.36 eV band is attributed to Cu_{Ga} , as noted in the previous sample. It should be noted that the intensity of this spectrum is very low, indicating probable severe surface damage.

At 10 keV the 1.514, 1.484, 1.468, and 1.432 eV bands are observed. The 1.484 is attributed to Si_{As} (Ref 1). The dominant peak, 1.468 eV, is thought to be V_{As} defect related as noted earlier. The 1.432 appears to be a LO phonon replica of the 1.468 eV band since it has a rough separation energy of 36 meV. It is noteworthy that this spectra is similar to the spectrum of Sample 2, except that Si_{As} has seemingly replaced the Zn_{As} peak and the intensity of this spectrum is an order of magnitude less. One should also note that the ion implant concentrations are different by an order of magnitude.

At 15 keV the 1.513, 1.495, 1.489, 1.470, 1.432, and 1.36 eV bands are observed. They have been previously attributed to unresolved excitons, C_{As} , Zn_{As} , V_{As} defect related, LO phonon replica, and Cu_{Ga} . At this maximum penetration depth of 1.1 μm , the dominant peak is observed to be due to Zn_{As} (1.489 eV). At this penetration depth, the luminescence intensity was found to be moderately high, surpassed only by (thermally annealed) Sample 3.

This spectrum closely approximates that of Sample 4. The main difference, aside from the luminescence intensities, is that this sample has a characteristic 1.468 eV V_{As} damage related peak. Since the luminescence intensity is moderately

high and this spectrum nearly coincides with that of Sample 4, one might contend that some laser annealing in this region took place. The criteria used here is that of high concentrations of radiative centers and low damage related peak intensities.

Comparing the spectra of the various penetration depths of this sample, one notes some interesting observations. At 5 keV the spectrum was characterized by the Ge_{As} (1.480 eV) and probable V_{As} diatomic donor or acceptor complex related (1.447 eV) peaks. At 10 keV a complete change took place. The spectrum was characterized by the Si_{As} (1.484 eV) and V_{As} damage related (1.468 eV) peaks. Then, at 15 keV, a change took place again. This time the spectrum was characterized by the Zn_{As} (1.489 eV) and V_{As} damage related (1.468 eV) peaks. These results seem to indicate that temperature plays a very important role in laser annealing, if indeed, temperature is responsible for the lattice vacancy competition among the various impurities.

Sample 10. Sample 10 was investigated using an electron beam energy of 10 keV at 10°K. The spectrum, shown on the next page in Fig 15, is characterized by only two main peaks of moderate luminescence intensity. These were the 1.489 eV peak attributed to Zn_{As} and the 1.409 eV peak attributed to V_{As} acceptor complexes. Lower energy, but unresolved, peaks were present. These contributed no useful information and were, therefore, not considered any further.

Especially noteworthy in this sample was the observation

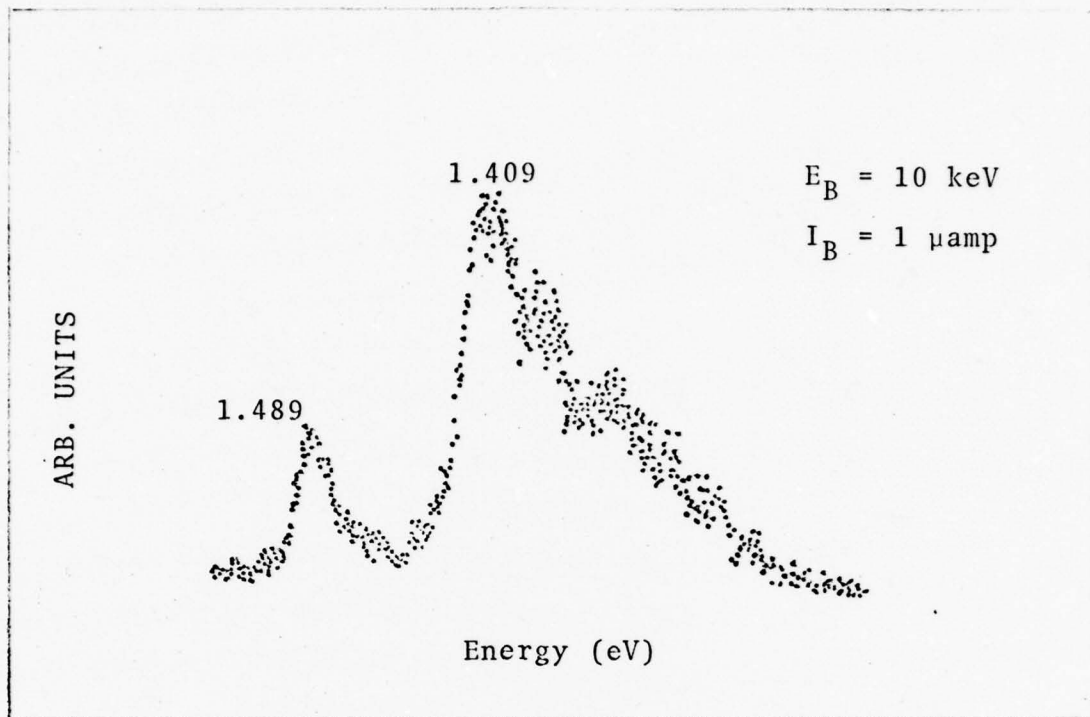


Fig 15. The CL Spectrum Obtained at 10°K on Sample 10

that above 1.409 eV, the non-radiative centers dominated the normally radiative centers, except at 1.489 eV.

This sample is similar to Sample 3 in the region of the 1.409 eV peak through lower energies. For energies above 1.409 eV, this sample is similar in that the 1.489 eV band is also found in Sample 3. The major difference between the two samples lies in the fact that this sample has no observed peaks at 1.478 eV or 1.455 eV. The lack of these peaks, attributed to Ge, seems to indicate the lack of sufficient laser annealing.

V. Conclusions and Recommendations

Conclusions

Cathodoluminescence was utilized to investigate germanium implanted GaAs with an emphasis on the effects of laser annealing. The laser annealed samples were provided from a thesis study performed concurrently with this experiment (Ref 37). Due to the magnitude of this research project, this study represents only a portion of the total effort to characterize Ge implanted-laser annealed GaAs. Therefore, any conclusions presented at this time are tentative and, in fact, are basically the significant observations obtained from the study. Presently, experimental data is still being collected, and a more complete set of conclusions concerning recombination theory of laser annealed Ge:GaAs is thus anticipated in the near future. The primary observations drawn from this study are the following:

(1) At 10 keV and 15 keV the U.A. sample was strongly characterized by the 1.47 eV V_{As} -defect related peak. At these same electron irradiation energies, the thermal annealed samples showed no evidence of the damage related 1.47 eV peak. The thermal annealed samples showed Ge related peaks. Although low in intensity, no Ge related peaks were observed in the U.A. implanted sample.

(2) At 10 keV and 15 keV the laser annealed implanted samples were characterized by extremely low luminescence in comparison to the thermal annealed samples. Additionally, the

spectra of the laser annealed samples were characterized by dominant 1.47 eV energy peaks.

The laser annealed sample spectra in comparison to the spectra of the unannealed samples were characterized by nearly the same energy peaks. Thus, it is highly suggested that due to the above noted observations, the laser anneal samples are not sufficiently annealed. Ge related energy peaks due to implant annealing were not observed in the laser annealed Ge implanted samples.

(3) The unimplanted laser annealed samples were characterized by very low to no detectable luminescence. When irradiated with 10 keV electrons, the luminescence of the samples was characterized by a dominant peak at 1.47 eV. Thus, the very low level of luminescence, coupled with the dominant 1.47 eV energy peak, strongly indicates a heavily damaged area in these samples within a depth of about 5400Å.

The secondary observations are the following:

(1) The laser annealed samples were characterized by severe surface damage. This fact was ascertained by noting the dramatic changes between spectral emissions obtained at 5 keV and those obtained at 10 and 15 keV. These results seem to indicate that the laser anneal temperature might play a very important role in the annealing process. Additionally, these results suggest that capping samples prior to laser annealing or etching the surface layer (approximately 1900Å) following the laser anneal process may be necessary.

(2) The 1.493 eV peak was observed only in the unannealed

samples and in the ($3E14$ and $3E13$) laser annealed samples (8 and 9). It is attributed to a C_{As} (F-B) recombination mechanism. The fact that C_{As} was observed in only laser annealed samples, and then only as a shoulder, suggests that annealing causes carbon to yield its radiation centers to another impurity.

(3) The 1.489 eV peak was present in all samples except Sample 1 and Sample 9 at 10 keV. This peak was attributed to a (F-B) Zn_{As} recombination mechanism. The presence of Zn_{As} in nearly all samples suggests that carbon yields its V_{As} to Zn during annealing or heavy ion dose implantations. In the case of the $3E13$ laser annealed sample (Sample 9), the 1.484 eV peak attributed to Si seems to have dominated the C and Zn previously controlled radiation centers. This peak remained essentially constant over an electron beam excitation energy range of 5-15 keV.

(4) The 1.479 eV peak was present only in the thermally annealed samples with a possible peak due to Ge traces observed in the unimplanted-unannealed sample. This peak is presently attributed to a (D-A) pair recombination involving Ge_{Ga} and Ge_{As} , but more experiments in temperature variation are required to confirm this contention. The presence of this peak only in the thermal annealed samples strongly suggests the possibility that the induced disorder and damage in the laser annealed implanted samples was not removed by the laser annealing. A second possibility is that the lattice order has been restored by the laser annealing but that the Ge ions did not move into substitutional sites.

(5) The 1.469 eV peak, attributed to damage related defects, was present in all but the thermally annealed samples and Sample 10. Again, this suggests the possibility of insufficient annealing in the laser annealed samples.

(6) The 1.455-9 eV peak, attributed to Ge, was present only in the thermal anneal samples. The literature indicates this peak to be attributed to a $V_{As}-Ge_{As}$ complex. Therefore, this peak appears to be possibly yet another indication of a fully annealed ion implanted sample.

(7) The 1.407-9 eV peak, attributed to V_{As} -acceptor complexes, was present only in the 3E13 thermal annealed sample and the second 3E13 laser annealed sample (Sample 10).

(8) The 1.36 eV peak was present in all non-laser annealed samples and in the 3E14 laser annealed sample. This appears to indicate the presence of Cu in most samples. Since no Cu peak was observed in Samples 5, 6, and 9, this probably indicates a lack of thermally generated gallium vacancies. This, of course, can be explained by the time frame in which the laser anneal process takes place.

(9) Probably the most notable of all observations is that concerning the dominant peaks (1.489 eV) in the thermal annealed samples. The spectral emissions of these samples were expected to reflect strong Ge peaks at 1.478 eV rather than at 1.489 eV.

In summary then, the following points should be noted. Due to observation (1), items (2) - (9) are the result of the spectral emissions generated by 10 keV and 15 keV electron beam

energies only. Also, the fact that Sample 7 presented no radiative luminescence information appears to be due to the extensive laser energy density deposited on this sample.

Recommendations

As a result of this study, several recommendations are suggested in areas requiring a more extensive research effort. These recommendations include the following:

(1) To provide additional evidence of the originating recombination mechanisms of the observed energy peaks, additional spectra emissions need to be obtained over different temperature ranges.

(2) Hall measurements should be made on the various samples to yield further evidence on the impurities responsible for the observed energy peaks.

(3) Because of the heavy surface damage on the laser annealed samples, it is highly recommended that the first approximate 1900Å layer be etched off and then to have the samples probed again. Sample 7, for example, may then be found to yield luminescence spectra.

(4) A wider range of fluences of unannealed, thermal annealed, and laser annealed samples should be examined.

(5) To provide additional insight into thermal annealed Ge implanted GaAs, it is recommended that the 1000Å Si₃N₄ caps be etched from such samples. This would allow deeper penetration of the electron beam for the energies used in this study. This would yield more information that would more clearly

delineate the trends of peak energies versus excitation energies. It would also yield much more information concerning the recombination mechanisms involving Ge.

Bibliography

1. Ashen, D.J. et al. "The Incorporation and Characterization of Acceptors in Epitaxial GaAs." Journal of Physics and Chemistry of Solids, 36:1041-1053 (1975).
2. Bass, J. C. "Gallium Arsenide Microwave Devices," in Gallium Arsenide and Related Compounds, 1970. Conference Ser. (9); The Institute of Physics (London and Bristol), 129-139 (1971).
3. Bok, J. "Preface," in Gallium Arsenide and Related Compounds, 1974. Conference Ser. (24), The Institute of Physics (London and Bristol). (1975).
4. Bolstov, V. V. et al. "Laser Annealing of Defects Responsible for Additional Optical Absorption in Ion-Implanted Gallium Arsenide." Soviet Physics of Semiconductors, 10:338-339 (March 1976).
5. Boulet, D. L. Depth Resolved Cathodoluminescence of Cadmium Implanted Gallium Arsenide, Unpublished Thesis, Wright-Patterson Air Force Base, Ohio: Air Force Institute of Technology (December 1975).
6. Boyd, G. V. Time-Resolved Cathodoluminescence of Cadmium Implanted Gallium Arsenide, Unpublished Thesis, Wright-Patterson Air Force Base, Ohio: Air Force Institute of Technology (June 1976).
7. Carter, G., et al. "Radiation Damage By Implanted Ions in GaAs and GaP." Radiation Effects, 6:277-284 (1970).
8. Chang, L. L. et al. "Vacancy Association of Defects in Annealed GaAs." Applied Physics Letters, 19:143-5 (1971).
9. Chatterjee, P. K., et al. "Photoluminescence Study of Native Defects in Annealed GaAs." Solid State Communications, 17:1421-24 (1975).
10. Chiang, S. Y. and G. L. Pearson. "Photoluminescence Studies of Vacancies and Vacancy-Impurity Complexes in Annealed GaAs." Journal of Luminescence, 10:313-322 (1975).
11. Coates, A. Gallium Arsenide and Related Compounds, 1971. Conference Ser. (23), The Institute of Physics (London and Bristol), 96 (1972).

12. Cone, M. L. Characterization of Ion-Implanted GaAs. Unpublished Dissertation, Wright-Patterson Air Force Base, Ohio: Air Force Institute of Technology (December 1978).
13. Dean, P. J. "Junction Electroluminescence." Applied Solid State Science, 1:1-151. Academic Press, New York and London; 1969.
14. Duchynski, R. J. "Ion Implantation For Semiconductor Devices." Solid State Technology, 20:53-58 (November 1977).
15. Dumoulin, J. D. Depth Resolved Cathodoluminescence on the Effects of Cd Implantation and Annealing in Gallium Arsenide. Unpublished Thesis, Wright-Patterson Air Force Base, Ohio: Air Force Institute of Technology (December 1976).
16. Gamo, K., et al. "Reordering of Implanted Amorphous Layers in GaAs." Radiation Effects, 33:85-89 (1977).
17. Gat, A. and J. F. Gibbons. "A Laser-Scanning Apparatus For Annealing of Ion-Implantation Damage in Semiconductors." Applied Physics Letters, 32:142-143 (February 1978).
18. Gibbons, J. F. "Ion Implantation in Semiconductors - Part I: Range Distribution Theory and Experiments." Proceedings of the IEEE, 56:295-319 (March 1968).
19. _____ . "Ion Implantation in Semiconductors - Part II: Damage Production and Annealing." Proceedings of the IEEE, 60:1062-1096 (September 1972).
20. _____ , et al. Projected Range Statistics. New York: Halstead Press, 1975.
21. Golovchenko, J. A. "Annealing of Te-Implanted GaAs By Ruby Laser Irradiation." Applied Physics Letters, 32: 147-149 (1978).
22. Harris, J. S. and F. H. Eisen. "The Annealing of Damage in Ion Implanted Gallium Arsenide." Radiation Effects, 7:123-128 (1971).
23. Heim, K. and P. Hiesinger. "Luminescence and Excitation Spectra of Exciton Emission in GaAs." Physical States of Solids, 66:461-470 (1974).
24. Hilsum, C. "Preface." Gallium Arsenide and Related Compounds, 1972. Conf. Ser. (17); The Institute of Physics (London and Bristol), 1973.

25. Hwang, C.J. "Photoluminescence Study of Thermal Conversion in GaAs grown from Silica Boats." Journal of Applied Physics, 39:5347-5356 (1968).
26. Ilegems, M. and R. Dingle. "Acceptor Incorporation in GaAs Grown by Beam Epitaxy." Gallium Arsenide and Related Compounds, 1974. Conference Ser. (23). The Institute of Physics (London and Bristol), 1975.
27. Kachurin, G.A. and E.V. Nidaev. "Effectiveness of Annealing of Implanted Layers by Millisecond Laser Pulses." Soviet Physics of Semiconductors, 11:1178-80 (October 1977).
28. _____, et al. "Annealing of Radiation Defects by Laser Radiation Pulses.: Soviet Physics of Semiconductors, 9:946 (1976).
29. _____, et al. "Proceedings of the Fifth International Conference on Ion Implantation in Semiconductors & Other Materials (1976)," Ed. by F. Chernov, J. Borders and D. Brice, Plenum Publishing Cor. (1977).
30. Kasano, H. "Diatomic-Complex Donor and Acceptor Model for Ge-Doped Vapor-Grown GaAs." Journal of Applied Physics, 49:4021-4030 (1978)
31. Khaibullin, I.B., et al. "Some Features of Laser Annealing in Ion Implanted Layers." Radiation Effects, 36:225-233 (1978).
32. Koschel, W.H., et al. "Photoluminescence Studies of Surface Degradation on Semi-Insulating GaAs Substrates During the LPE Growth Cycle." Gallium Arsenide and Related Compounds, 1976. Conference Ser. (33a). The Institute of Physics (London and Bristol) 98-104 (1977).
33. Kressel, H. "Luminescence Due to Ge Acceptors in GaAs." Journal of Applied Physics, 39:4059-4066 (1968).
34. Lidow, A., et al. "Fast Diffusion of Elevated-Temperature Ion-Implanted Se in GaAs as Measured by Secondary Ion Mass Spectrometry." Applied Physics Letters, 32:149-151 (February 1978).
35. Lum, W.Y. and H.H. Wieder. "Thermally Converted Surface Layers in Semi-Insulating GaAs." Applied Physics Letters, 31:213-215 (August 1977).
36. _____, et al. "Epilayer-Substrate Interfaces of Ge-Doped GaAs Grown by Liquid Phase Epitaxy." Journal of Applied Physics, 49:3333-3336 (June 1978).

37. Martinelli, R.U., and C.C. Wang. "Electron-Beam Penetration in GaAs." Journal of Applied Physics, 44: 3350-3351 (July 1973).
38. Mason, R.S. Laser Annealing of Ion Implanted Gallium Arsenide. Unpublished Thesis, Wright-Patterson Air Force Base, Ohio: Air Force Institute of Technology (December 1978).
39. Norris, C.B., et al. "Depth-Resolved Cathodoluminescence in Undamaged and Ion-Implanted GaAs, ZnS and CdS." Journal of Applied Physics, 44:3209-3221 (July 1973).
40. Pierce, B.J. "Luminescence and Hall Effect of Ion Implanted Layers in ZnO." Unpublished Dissertation, Wright-Patterson Air Force Base, Ohio: Air Force Institute of Technology (September 1974).
41. _____ . "Time Resolved Spectroscopy of ZnSe." Unpublished Thesis, Wright-Patterson Air Force Base, Ohio: Air Force Institute of Technology (June 1969).
42. Rimini, E., et al. "Laser Pulse Energy Dependence of Annealing in Ion Implanted Si and GaAs Semiconductors." Physics Letters, 65A:153-155 (February 1978).
43. Rosztochy, F.E., et al. "Germanium-Doped GaAs." Journal of Applied Physics, 41:264-270 (January 1970).
44. Sansbury, J. "Applications of Ion Implantation in Semiconductor Processing." Solid State Technology, 19: 31-37 (November 1976).
45. Sell, D.D., et al. "Polariton Reflectance and Photoluminescence in High-Purity GaAs." Physical Review B, 7:4568-4586 (May 1973).
46. Schairer, W. and W. Graman. "Photoluminescence of Ge Doped GaAs Grown by Vapor-Phase-Epitaxy." Journal of Physics and Chemistry of Solids, 30:2225-2229 (1969).
47. _____ , and T.O. Yep. "Two-Hole Transitions in the Luminescence of Excitons Bound to Neutral Acceptors in GaAs." Solid State Communications, 9:421-424 (1971).
48. Smith, R.A. Semiconductors. Cambridge: University Press, 1959.
49. Stocker, H.J. and M. Schmidt. "Photoluminescence of the Cr Acceptor in Boat-Grown and LPE GaAs." Journal of Applied Physics, 47:2450-2451 (June 1976).

50. Summers, C.J., et al. "Far-Infrared Donor Absorption and Photoconductivity in Epitaxial n-Type GaAs." Physical Review B, 1:1603-1606 (February 1970).
51. Sze, S.M. Physics of Semiconductor Devices. New York: Wiley-Interscience, 1969.
52. Walter, M.J. "Depth Resolved Cathodoluminescence of Carbon Implanted Gallium Arsenide." Unpublished Thesis Wright-Patterson Air Force Base, Ohio: Air Force Institute of Technology (December 1977).
53. White, A.M., et al. "Acceptor Levels in Gallium Arsenide." Journal of Physics C: Solid State Physics, 6:L243-L246 (1973).
54. Williams, E.W. "A Photoluminescence Study of Acceptor Centers in GaAs." British Journal of Applied Physics, 18:253-262 (1967)
55. _____, and C.T. Elliot. "Luminescence Studies of a New Line Associated with Germanium in GaAs." British Journal of Applied Physics (Journal of Physics D), Series 2(12):1657-1665 (1969).
56. _____, and H.B. Bebb. "Photoluminescence II: Gallium Arsenide." Semiconductors and Semimetals, VIII: 321-391 (1972).
57. Woodcock, J.M., et al. "Electrical and Cathodoluminescence Measurements on Ion Implanted Donor Layers in GaAs." Solid State Electronics, 18:267-275 (1975).
58. Young, R.T., et al. "Laser Annealing of Boron-Implanted Silicon." Applied Science Letters, 32:139-141 (February 1978).

APPENDIX A

GaAs Values of Interest

<u>Band Gap (E_g)</u>		
10°K	1.521	1
300°K	1.43	1
<u>Dielectric Constant(ε)</u>		
	10.9	1
	12.5	2
<u>Absorption Coefficient (α)</u>		
He-Ne laser line	4.6 x 10 ⁴ cm ⁻¹ at 2 eV	3
Ruby laser line	2 x 10 ⁴ cm ⁻¹ at 1.7857 eV	4
5 - 2μ = λ for SI GaAs	0.3 - 0.5 cm ⁻¹ at .24-.62 eV	5
5 - 2μ = λ for Te:GaAs (unannealed)	5 x 10 ³ cm ⁻¹ at .248-.62 eV	5
<u>Donor Energy (E_D)</u>		
	6.0	6
	6.08	7
<u>Acceptor Energy (E_A)</u>		
Isolated, atomic complexes	30,70 meV	8
Hall measurements, photoluminescence	35,38 meV	9
Epitaxial GaAs layers	41.2 meV	10
Vapor Phase Epitaxy, T ≤ 20°K	42±1 meV	11
<u>Density of GaAs</u>		
	5.3 g/cm ³	12

¹(Ref 51:20)

²(Ref 50:1603)

³(Ref 22:123)

⁴(Ref 28:946)

⁵(Ref 4:339)

⁶(Ref 46:2228)

⁷(Ref 50:1603)

⁸(Ref 33:4059)

⁹(Ref 43:264)

¹⁰(Ref 53:L243)

¹¹(Ref 46:2227)

¹²(Ref 28:946)

APPENDIX B

Various Estimates of Electron Beam Penetrations

Beam Energy (keV)	Depth ¹ (μm)	Depth ² (μm)	Depth ³ (μm)	Greatest Loss ³ (μm)
5	.1400	.283	.1960	.0245
7.5		.5116		
10	.4800	.7780	.5392	.0735
13		1.1420		
15		1.4075	1.1275	.1078
20	1.6000	1.6897	1.7156	.147

¹(Ref 39:3210)

²(Ref 37:3351)

³(Ref 12)

Vita

James H. Walcher was born on 19 January 1945 in Denver, Colorado. He graduated from Wayne High School at Dayton, Ohio in 1963. In 1967, after spending nearly four years in the Air Force, James Walcher entered college at Southwestern State University in San Marcos, Texas. In 1970, he graduated with a B.S. degree in Physics and entered the Air Force's Officer Training School (OTS). Upon completion of OTS, he went on to Undergraduate Navigator Training. Capt. Walcher went into C130's upon graduation and flew missions throughout Southeast Asia, the Pacific area, and Europe. In June 1977, Capt. Walcher began his tour at the Air Force Institute of Technology in Dayton, Ohio in order to obtain his M.S. degree in Physics.

Permanent address: 16668 Forest Way
Austin, Texas 78734

UNCLASSIFIED

SECURITY CLASSIFICATION OF THIS PAGE (When Data Entered)

REPORT DOCUMENTATION PAGE		READ INSTRUCTIONS BEFORE COMPLETING FORM
1. REPORT NUMBER AFIT/GEP/PH/78D-16	2. GOVT ACCESSION NO.	3. RECIPIENT'S CATALOG NUMBER
4. TITLE (and Subtitle) CATHODOLUMINESCENCE OF GERMANIUM IMPLANTED GALLIUM ARSENIDE AND THE EFFECTS OF LASER ANNEALING		5. TYPE OF REPORT & PERIOD COVERED MS Thesis
		6. PERFORMING ORG. REPORT NUMBER
7. AUTHOR(s) James H. Walcher Capt USAF		8. CONTRACT OR GRANT NUMBER(s)
9. PERFORMING ORGANIZATION NAME AND ADDRESS Air Force Institute of Technology (AFIT-ENA) Wright-Patterson AFB, OH 45433		10. PROGRAM ELEMENT, PROJECT, TASK AREA & WORK UNIT NUMBERS Project No. 2306 Work Unit No. R2-13
11. CONTROLLING OFFICE NAME AND ADDRESS AF Avionics Laboratory Wright-Patterson AFB, OH 45433		12. REPORT DATE December 1978
		13. NUMBER OF PAGES 72
14. MONITORING AGENCY NAME & ADDRESS (if different from Controlling Office)		15. SECURITY CLASS. (of this report) Unclassified
		15a. DECLASSIFICATION/DOWNGRADING SCHEDULE
16. DISTRIBUTION STATEMENT (of this Report) Approved for public release; distribution unlimited		
17. DISTRIBUTION STATEMENT (of the abstract entered in Block 20, if different from Report)		
18. SUPPLEMENTARY NOTES Approved for public release; IAW AFR 190-17 JOSEPH P. HIPPS, MAJ, USAF Director of Information 1-23-79		
19. KEY WORDS (Continue on reverse side if necessary and identify by block number) III-V Compounds Cathodoluminescence Gallium Arsenide Laser Annealing Germanium Implant		
20. ABSTRACT (Continue on reverse side if necessary and identify by block number) The primary objective of this study was to characterize experimental laser annealed samples using cathodoluminescence. Ten Cr-doped (SI) GaAs samples were studied. These samples included an unimplanted-unannealed sample, several unimplanted but laser annealed samples, Ge implanted (fluence of 3×10^{13} ions/cm ² and 3×10^{14} ions/cm ²) thermally annealed and laser annealed samples, and a Ge implanted (fluence of 3×10^{14} ions/cm ²) unannealed sample. The results indicated the experimental laser annealed samples to be partially or completely		

DD FORM 1 JAN 73 1473

EDITION OF 1 NOV 65 IS OBSOLETE

UNCLASSIFIED

SECURITY CLASSIFICATION OF THIS PAGE (When Data Entered)

UNCLASSIFIED

SECURITY CLASSIFICATION OF THIS PAGE(When Data Entered)

unannealed. The laser annealed samples were generally characterized by weak luminescence with peaks at 1.514 eV due to unresolved excitons, 1.488 eV attributed to Zn_{As} , and 1.469 eV (damage related). It was further observed that in the thermally annealed samples, the dominant peak was noted at 1.488 eV instead of the expected 1.478 eV peak previously associated with Ge. Finally, the unannealed sample spectra emissions were characterized by a 1.493 eV peak attributed to C_{As} , and in all non-laser annealed samples a 1.36 eV peak attributed to Cu_{Ga} was observed.

UNCLASSIFIED

SECURITY CLASSIFICATION OF THIS PAGE(When Data Entered)